

Application of meteorology-based methods to determine local and external contributions to particulate matter pollution: A case study in Venice (Italy)

Squizzato, Stefania; Masiol, Mauro

DOI:

[10.1016/j.atmosenv.2015.08.026](https://doi.org/10.1016/j.atmosenv.2015.08.026)

License:

Creative Commons: Attribution-NonCommercial-NoDerivs (CC BY-NC-ND)

Document Version

Peer reviewed version

Citation for published version (Harvard):

Squizzato, S & Masiol, M 2015, 'Application of meteorology-based methods to determine local and external contributions to particulate matter pollution: A case study in Venice (Italy)', *Atmospheric Environment*, vol. 119, pp. 69-81. <https://doi.org/10.1016/j.atmosenv.2015.08.026>

[Link to publication on Research at Birmingham portal](#)

General rights

Unless a licence is specified above, all rights (including copyright and moral rights) in this document are retained by the authors and/or the copyright holders. The express permission of the copyright holder must be obtained for any use of this material other than for purposes permitted by law.

- Users may freely distribute the URL that is used to identify this publication.
- Users may download and/or print one copy of the publication from the University of Birmingham research portal for the purpose of private study or non-commercial research.
- User may use extracts from the document in line with the concept of 'fair dealing' under the Copyright, Designs and Patents Act 1988 (?)
- Users may not further distribute the material nor use it for the purposes of commercial gain.

Where a licence is displayed above, please note the terms and conditions of the licence govern your use of this document.

When citing, please reference the published version.

Take down policy

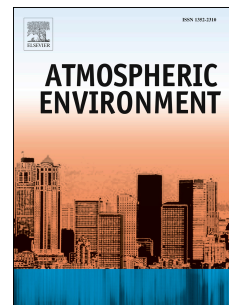
While the University of Birmingham exercises care and attention in making items available there are rare occasions when an item has been uploaded in error or has been deemed to be commercially or otherwise sensitive.

If you believe that this is the case for this document, please contact UBIRA@lists.bham.ac.uk providing details and we will remove access to the work immediately and investigate.

Accepted Manuscript

Application of meteorology-based methods to determine local and external contributions to particulate matter pollution: A case study in venice (Italy)

Stefania Squizzato, Ph.D., Mauro Masiol



PII: S1352-2310(15)30271-5

DOI: [10.1016/j.atmosenv.2015.08.026](https://doi.org/10.1016/j.atmosenv.2015.08.026)

Reference: AEA 14009

To appear in: *Atmospheric Environment*

Received Date: 23 April 2015

Revised Date: 7 August 2015

Accepted Date: 10 August 2015

Please cite this article as: Squizzato, S., Masiol, M., Application of meteorology-based methods to determine local and external contributions to particulate matter pollution: A case study in venice (Italy), *Atmospheric Environment* (2015), doi: 10.1016/j.atmosenv.2015.08.026.

This is a PDF file of an unedited manuscript that has been accepted for publication. As a service to our customers we are providing this early version of the manuscript. The manuscript will undergo copyediting, typesetting, and review of the resulting proof before it is published in its final form. Please note that during the production process errors may be discovered which could affect the content, and all legal disclaimers that apply to the journal pertain.

1
2
3
4
5
6 **APPLICATION OF METEOROLOGY-BASED**
7 **METHODS TO DETERMINE LOCAL AND**
8 **EXTERNAL CONTRIBUTIONS TO**
9 **PARTICULATE MATTER POLLUTION: A**
10 **CASE STUDY IN VENICE (ITALY)**

11
12 **Stefania Squizzato^{1*}, Mauro Masiol²**

13
14
15 **¹Dipartimento di Scienze Ambientali, Informatica e Statistica,**
16 **Università Ca' Foscari Venezia, Dorsoduro 2137, IT-30123**
17 **Venezia, Italy**

18 **²Division of Environmental Health and Risk Management**
19 **School of Geography, Earth and Environmental Sciences**
20 **University of Birmingham**
21 **Edgbaston, Birmingham B15 2TT**
22 **United Kingdom**

23
24
25
26
27
28 ***Corresponding author:**

29 Stefania Squizzato, Ph.D.

30 Dipartimento di Scienze Ambientali, Informatica e Statistica, Università Ca' Foscari Venezia,
31 Dorsoduro 2137, 30123 Venice, Italy

32 E-mail: stefania.squizzato@unive.it; stefania.squizzato81@gmail.com

33 Tel: +39 041 2348639

34 **ABSTRACT**

35 The air quality is influenced by the potential effects of meteorology at meso- and synoptic scales.
36 While local weather and mixing layer dynamics mainly drive the dispersion of sources at small
37 scales, long-range transports affect the movements of air masses over regional, transboundary and
38 even continental scales. Long-range transport may advect polluted air masses from hot-spots by
39 increasing the levels of pollution at nearby or remote locations or may further raise air pollution
40 levels where external air masses originate from other hot-spots. Therefore, the knowledge of
41 ground-wind circulation and potential long-range transports is fundamental not only to evaluate
42 how local or external sources may affect the air quality at a receptor site but also to quantify it.
43 This review is focussed on establishing the relationships among $PM_{2.5}$ sources, meteorological
44 condition and air mass origin in the Po Valley, which is one of the most polluted areas in Europe.
45 We have chosen the results from a recent study carried out in Venice (Eastern Po Valley) and have
46 analysed them using different statistical approaches to understand the influence of external and
47 local contribution of $PM_{2.5}$ sources. External contributions were evaluated by applying Trajectory
48 Statistical Methods (TSMs) based on back-trajectory analysis including (i) back-trajectories cluster
49 analysis, (ii) potential source contribution function (PSCF) and (iii) concentration weighted
50 trajectory (CWT). Furthermore, the relationships between the source contributions and ground-wind
51 circulation patterns were investigated by using (iv) cluster analysis on wind data and (v) conditional
52 probability function (CPF). Finally, local source contribution have been estimated by applying the
53 Lenschow' approach.

54 In summary, the integrated approach of different techniques has successfully identified both local
55 and external sources of particulate matter pollution in an European hot-spot affected by the worst
56 air quality.

57
58 **Keywords: $PM_{2.5}$, local and external contributions, meteorology-based methods**

59
60
61
62
63
64
65
66
67
68

1. INTRODUCTION

Since mid 90s, the European Community has adopted increasingly stringent standards for reduction of emissions to improve air quality. Such efforts have generally led to an overall improvement of air quality in most of the EU Countries. However, there are still some European regions that are affected by high levels of air pollutants - the so-called hot-spots. Among others, Northern Italy, Benelux, some Eastern Countries and greater urban areas such London and Paris deserve particular attention because of their high population density.

Generally, the main causes of high air pollution levels in hot-spots are the additive effects of: (i) heavy local emissions from many anthropogenic sources; (ii) peculiar weather and/or orographic features limiting the dispersion of locally emitted pollutants and (iii) the regional or even trans-boundary transport of polluted air masses from external source areas. The first cause is primarily related to the levels of urbanization and industrialization: since most hot-spots lie in densely anthropised areas which are affected by relatively heavy emissions from traffic, energy production and industrial activities. Beyond the local emission sources, air quality may be further influenced by the potential effects of meteorology at meso- and synoptic scales. While local weather and mixing layer dynamics mainly drive the dispersion of sources at small scales, long-range transports affect the movements of air masses over regional, trans boundary and even continental scales and may have two opposite but potentially concurrent effects: (i) they can advect polluted air masses from hot-spots by increasing the level of pollution at near areas or even remote locations, and/or (ii) they may further raise air pollution levels where external air masses originate from other hot-spots.

Therefore, the knowledge of ground-wind circulation and potential long-range transports is essential to evaluate how and how much local or external sources may affect the air quality at a receptor site.

The main goal of this study is to establish a relationship among $PM_{2.5}$ sources, meteorological condition and air mass origin through the application of a multiple methods and tools. The results of a recent source apportionment study carried out in Venice (Eastern Po Valley) over three sites were evaluated using various statistical approaches to determine the influence of external and local contribution on identified $PM_{2.5}$ sources. External contributions were evaluated by applying Trajectory Statistical Methods (TSMs) based on back-trajectory analysis: (i) back-trajectories cluster analysis; (ii) potential source contribution function (PSCF) and (iii) concentration weighted trajectory (CWT). Furthermore, the relationships between the source contributions and ground-wind circulation patterns were investigated using (iv) cluster analysis on wind data and (v) conditional probability function (CPF). Finally, local source contributions have been estimated following the approach proposed by Lenschow et al. (2001).

The application of multiple techniques has identified both local and external sources of particulate matter pollution in an European hot-spot affected by worst air quality. We strongly believe that the

104 proposed approaches will be useful for the future air quality assessment studies and reduction
105 strategies.

106

107 **2. MATERIALS AND METHODS**

108 *2.1 Study area*

109 While Northern Italy has fulfilled the same mitigation processes adopted by other European
110 Countries towards emissions reduction, it has not fully benefited in terms of substantial reduction of
111 air pollution. As of today, the Po Valley is one of the most polluted areas in the Europe for
112 particulate matter (PM), ozone and nitrogen oxides (EEA, 2015). Local emissions are expected to
113 be more important in Po Valley than in other European areas (Maurizi et al., 2013) although
114 Gilardoni et al. (2011) showed that local sources mainly affect fine PM (aerodynamic diameter less
115 than $2.5\ \mu\text{m}$, $\text{PM}_{2.5}$) during winter while the influence of regional air masses from the nearby Po
116 Valley dominates in summer. Moreover, the generation of secondary aerosol is known to form over
117 the Valley that rapidly build-up air pollution after clean-air episodes which is governed by the
118 particular topology and meteorological conditions of the plain (Larsen et al., 2012; Masiol et al.,
119 submitted).

120 Venice is located between the eastern edge of the Po Valley and the Adriatic Sea. Along with the
121 city of Mestre, they form a large coastal urban municipality hosting 270,000 inhabitants. The
122 emission scenario includes sources of PM such as high density residential areas, heavy traffic roads
123 mostly congested during peak hours, a motorway and a motorway-link part of the main European
124 routes E55 and E70, an extended industrial area (Porto Marghera) with a large number of different
125 installations, including incineration plants and a large thermoelectric power plant burning coal and
126 refuse-derived fuel, the artistic glassmaking factories in the island of Murano, heavy shipping traffic
127 providing public/commercial and tourist transports and an international airport. The apportionment
128 of the most relevant PM sources and their spatial and seasonal changes (Masiol et al., 2012a;2014b)
129 as well as the regional and local influence of PM and secondary aerosol have been investigated
130 (Squizzato et al., 2012; Masiol et al., submitted). Moreover, the potential influence of local or long-
131 range transports upon PM mass and PM-bound pollutants were investigated in a series of sparse
132 studies (e.g., Masiol et al., 2010; 2012a,b; Squizzato et al., 2012; 2014), but its role on standard
133 breaching has not yet comprehensively assessed.

134 *2.2 Experimental*

135 A year-long $\text{PM}_{2.5}$ sampling campaign (February 2009 - January 2010) was carried out at the three
136 sites indicative of different environments (Fig. 1):

- 137 • a semi-rural background coastal site (SRB) installed on a coastal lighthouse upwind of the major
138 local emission sources;
- 139 • an urban background site (URB) established in a high density residential zone of Mestre, very
140 close (~50 m) to the main traffic roads;
- 141 • an industrial site (IND) placed downwind of Porto Marghera and the surrounding area that has
142 extensive road and shipping traffic.

143 Four time periods were selected for chemical analysis: spring (March-April 2009), summer (June-
144 July 2009), autumn (September-October 2009) and winter (December 2009-January 2010). Filters
145 were cut into two portions: one to determine major inorganic ions via ion exchange chromatography
146 (IC) (after water extraction) and the second to quantify elements via ICP-OES and ICP-MS after
147 acid digestion. Analytical methods are reported elsewhere (Squizzato et al., 2012; 2014).

148 Common weather data including wind speed and direction, air temperature, relative humidity, solar
149 radiation and precipitations were hourly measured at two stations near the sampling sites (Fig. 1):
150 ARPAV Cavallino-Treporti was chosen as being representative of SRB, while EZI5 (part of the
151 network of Ente della Zona Industriale di Porto Marghera) for URB and IND. Wind data were
152 homogenized and appropriate corrections were applied when necessary. The wind speeds $< 0.5 \text{ m}$
153 s^{-1} (anemometer detection limit) were assumed as calm wind whereas uncertain data or hours with
154 fast changes in wind direction were excluded from the analysis.

155 *2.3 Overview of back-trajectories and trajectory-based models*

156 There are number of methods that are currently used in air pollution studies to account for long-
157 range transports (Fleming et al., 2012 and references therein). Back-trajectory analysis is a
158 commonly-used tool for tracing the history of air masses passing over a location at a defined time.
159 Briefly, interpolated measured or modelled meteorological fields are used to infer backward in time
160 the most probable paths of infinitesimally small particles of air that at the time zero are located at a
161 starting point. In this study, back-trajectories were computed using HYSPLIT (Draxler and Rolph,
162 2015; Rolph, 2015). Our model set-up parameters included 4 days (-96 h) run time, starting height
163 of 20 m AGL, NCEP/NCAR Reanalysis data fields.

164 It is important to stress that back-trajectories are potentially associated with large uncertainties
165 (Stohl, 1998) mostly due to the oversimplification of the atmosphere in that dispersion is not
166 accounted for. Moreover, back-trajectories may be highly variable when run at different hours in a
167 day, causing further uncertainty when associated with daily pollutant data. To overcome large
168 uncertainties, the confidence of back-trajectories was tested using different starting heights and
169 hours: errors associated with a single trajectory were reduced by simulating four trajectories for
170 each sampling day (at 3:00, 9:00, 15:00 and 21:00). Taking into account the range of associated

171 uncertainties, the use of multiple trajectory-based models over long periods may yield more robust
172 results than the use of individual trajectories and may provide useful information about the external
173 source areas.

174 Back-trajectory modelling combined with atmospheric concentrations measured at the receptor site
175 are commonly referred to Hybrid Receptor Models (HRMs) (Han et al., 2007) or Trajectory
176 Statistical Methods (TSMs) (Kabashnikov et al., 2011; Brereton and Johnson, 2012). Most used
177 TSMs are: Potential Source Contribution Function (PSCF) (Hsu et al., 2003; Pekney et al., 2006;
178 Kim et al., 2005; Gildemeister et al., 2007; Han et al., 2007), Gridded Frequency Distributions
179 (GFD) (Weiss-Penzias et al., 2011), Concentration Fields Analysis (Rutter et al., 2009),
180 Concentration-Weighted Trajectory (CWT) (Seibert et al., 1994) and Residence Time Weighted
181 Concentration (RTWC) (Hsu et al., 2003; Han et al., 2007). All these methods essentially count the
182 frequency of back-trajectory segment endpoints in grid cells that make up the geographical domain
183 of interest for the receptor site (Cheng et al., 2013).

184 In this study three methods have been used, moreover an approach to determine the uncertainties
185 associated with PSCF is also proposed. Details of each method are provided as supplementary
186 material:

- 187 • *Cluster analysis on back-trajectories*: the principal purpose of back trajectories clustering is
188 to group trajectories having similar geographic origins and histories. The subsequent
189 coupling of clusters with chemical data associated to air pollutants is a simple but powerful
190 way to infer insights into the potential contribution of long-range transports from different
191 pathways.
- 192 • *PSCF*: It was initially developed to identify the likely locations of the regional PM sources
193 (Lee and Hopke, 2006; Pekney et al., 2006) and calculates the probability that a source is
194 located at latitude i and longitude j . The basis of PSCF is that if a source is located at
195 coordinates i and j , an air parcel back-trajectory passing through that location indicates that
196 material from the source can be collected and transported along the trajectory to the receptor
197 site. The PSCF value can be interpreted as the conditional probability that concentrations
198 larger than a given criterion value are related to the passage of air parcels through a grid cell
199 with this PSCF value during transport to the receptor site (Hsu et al., 2003). This method is
200 deficient in the determination of the statistical significance of its outcome and is suitable for
201 identifying possible source regions (Dvorska et al., 2008 and references therein). Generally,
202 PSCF values of 0.00–0.50 are considered as low whereas the values of 0.51–1.00 are
203 considered as high.
- 204 • *CWT*: the concentration weighted trajectory is a method of weighting trajectories with
205 associated concentrations (Hsu et al., 2003). In this procedure, each grid cell gets a weighted

206 concentration obtained by averaging sample concentrations that have associated trajectories
207 that crossed that grid cell as follows, i.e. each concentration is used as a weighting factor for
208 the residence times of all trajectories in each grid cell and then divided by the cumulative
209 residence time from all trajectories (Hsu et al., 2003; Cheng et al., 2013). In summary,
210 weighted concentration fields show concentration gradients across potential sources and
211 highlight the relative significance of potential sources (Hsu et al., 2003).

- 212 • *Evaluation of the uncertainties associated with PSCF*: despite the scientific literature
213 proposes different methods, at today there is not a unique standardized technique for
214 assessing the better estimates of the PSCF probabilities and their uncertainties. For example,
215 Pekney et al. (2006) used weighting functions multiplied by PSCF values for reducing the
216 effect of spurious large ratios in grid cells, while Lupu and Maenhaut (2002) and Hopke et
217 al. (1995) applied bootstrap techniques to estimate the statistical significance and the
218 uncertainties of the calculated PSCF values, respectively. Bootstrapping is not yet
219 implemented in the Openair package, however the package used weighted PSCF values
220 depending on the number of values in each cell (weights factors range from 0.15 to 2). The
221 bootstrapping techniques are widely used in chemometrics and provide accurate tools for
222 yielding estimates in cases where other methods are simply not available (Wehrens et al.,
223 2000). This way, the uncertainties associated to PSCF values in this study were estimated
224 externally by using a non-parametric bootstrap method. Briefly, $n=500$ subsamples
225 including 80% of the total number of trajectories were re-sampled without replacement from
226 the original dataset and PSCF was then re-run for each subsample. The 500 new PSCFs
227 maps were then merged to assess the average values and their associated standard deviations
228 for each cell in the grid domain. The uncertainties over the average results were then
229 expressed as average \pm standard deviation.

231 2.4 Overview of wind-based methods

232 The effectiveness of coupling air pollution data with wind data fields for identifying and accounting
233 local sources was largely demonstrated in a number of studies using very different approaches and
234 techniques (e.g., Ashbaugh et al., 1985; Kaufmann and Whiteman, 1999; Kim et al., 2003; Carslaw
235 et al., 2006; Viana et al., 2006; Masiol et al., 2012a; Uria-Tellaetxe and Carslaw, 2014). Such
236 approaches are based on the assumption that air pollutants emitted from a source are transported by
237 local winds. As a consequence, the levels of pollution recorded at a receptor site under downwind
238 conditions from the source should be higher when air blows from different sectors. However, these
239 methods generally disregard many issues linked to the dispersion of pollutants in the atmosphere,
240 e.g., the influence of atmospheric stability and turbulence on dilution of pollutants, the effects of the

241 mixing layer height on wind dynamics, the concentration-wind speed dependencies for certain
242 pollutants, the street canyon and urban canopy layer effects, etc. Despite the limitations, methods
243 for coupling air pollution with wind data are very useful in extracting information on local source
244 contributions and locations. Wind-based methods applied in this study aim to couple source
245 apportionment results with local wind fields recorded at ground:

- 246 • *Cluster of wind data*: The hourly data of wind speed and direction from the weather station
247 were processed by extracting their scalar components u and v relative to the North–South
248 and West–East axes (Kaufmann and Whiteman, 1999; Darby, 2005). In this study the hourly
249 values of the components were separately summed to obtain daily data, which represents the
250 resultant vector of the air movement. A hierarchical cluster analysis using the Ward's
251 method and the squared Euclidean distance measure were then performed on these
252 components.
- 253 • *CPF*: the conditional probability function (Kim et al., 2003; Kim and Hopke, 2004) analyses
254 local source impacts from varying wind directions using the source contribution estimates
255 from PMF coupled with the time-resolved wind directions. The CPF estimates the
256 probability that a given source contribution from a given wind direction will exceed a
257 predetermined threshold criterion. The sources are likely to be located at the directions that
258 have high conditional probability values (Kim et al., 2005). Details are reported as
259 supplementary material.

260

261 2.5 Lenschow approach

262 Local contributions can be estimated using the method proposed by Lenschow et al. (2001). Briefly,
263 the method essentially compares the PM levels and components (PMF sources, in this case)
264 measured in sites affected by different emission scenarios (semi-rural, urban and industrial, in this
265 case). In this study we assumed that: (i) the differences of particulate matter and its chemical
266 components between URB and IND can be attributed to the local influence of urban and industrial
267 area, respectively and (ii) SRB represents a rural background station affected by regional sources
268 with little contribution from the urban and industrial area. Only URB and IND samples with higher
269 concentration than SRB have been considered.

270

271 4. RESULTS AND DISCUSSION

272 4.1 Overview on PMF results

273 A multiple-site positive matrix factorization receptor model was performed over 448 PM_{2.5} samples
274 and 19 variables. Details of adopted methods and results are exhaustively reported in Masiol et al.
275 (2014b). Six factors associated with potential sources were extracted and apportioned, namely:

- 276 • secondary sulphate (made up of SO_4^{2-} and NH_4^+);
- 277 • ammonium nitrate and combustions (NO_3^- , NH_4^+ plus combustion tracers K^+ and Cl^-)
- 278 linked to gas-to-particles conversion processes involving NH_3 and NO_x (emitted both from
- 279 industries and traffic) and various combustion processes: K^+ was associated to biomass
- 280 combustion processes (Kundu et al., 2010) and the association K^+ - Cl^- was attributed to
- 281 gasoline vehicle emissions (Spencer et al., 2006);
- 282 • fossil fuels (V, Ni);
- 283 • traffic, mainly related to primary traffic emissions and road dust resuspension (Fe, Ti, Mn,
- 284 Cu, Ba, Mg^{2+});
- 285 • industrial (Zn, Pb, Mg^{2+});
- 286 • glassmaking (As, Cd).

287 The quantification of sources revealed that on annual basis the most impacting source in all the sites

288 is ammonium nitrate and combustions, accounting for $\sim 12 \mu\text{g m}^{-3}$ at all the sites, i.e. 47% of the

289 $\text{PM}_{2.5}$ mass in SRB and 38 % in URB and IND. Ammonium sulphate is the second largest

290 contributor, accounting for $5.6 \mu\text{g m}^{-3}$ (24 % in SRB and 17 % in URB and IND sites). As a matter

291 of fact, such sources account for most of the $\text{PM}_{2.5}$ mass (71% in SRB and 55% in URB and IND)

292 and their mass contributions are identical at all the sites, indicating that they are homogeneously

293 distributed throughout the area.

294

295 On the contrary, the remaining sources show different and variable contributions at the three sites.

296 This result is an early indication of their potential strong component of local origin: industrial

297 source contributes $7.1 \mu\text{g m}^{-3}$ in IND, $4.8 \mu\text{g m}^{-3}$ in URB and $3.6 \mu\text{g m}^{-3}$ in SRB, followed by road

298 traffic ($5.5 \mu\text{g m}^{-3}$ in URB, $3.3 \mu\text{g m}^{-3}$ in IND and $0.6 \mu\text{g m}^{-3}$ in SRB), fossil fuels ($2.9 \mu\text{g m}^{-3}$ in

299 IND, $2.1 \mu\text{g m}^{-3}$ in URB and $1.9 \mu\text{g m}^{-3}$ in SRB) and glassmaking ($1.7 \mu\text{g m}^{-3}$ in URB, $1.1 \mu\text{g m}^{-3}$

300 in IND and $1 \mu\text{g m}^{-3}$ in SRB).

301

302 *4.2 Results of trajectory-based methods*

303 Seven clusters are identified using the measure of the Euclidean distance and are named according to

304 their common origin. Five clusters are linked to long-range transports from Atlantic, Central

305 Europe, Northern Europe, Eastern EU and Western Mediterranean. Remaining two clusters are

306 associated with more local transports from East-Austria and from South/Central Italy. Fig. 1 shows

307 the frequency of trajectories passing through the grid cells in the grid domain and the average

308 trajectories associated to each identified cluster. The number of trajectories in each cluster is

309 reported in Table 1: a large number of trajectories pass over the Po Valley or blow from East-

310 Europe. These latter two clusters depict the two overwhelming pathways during the sampling

311 campaign. The potential effects of long-range/regional transports are then assessed by averaging the
312 levels of $PM_{2.5}$ and source contributions overall the study period: Table 1 reports the average
313 concentrations calculated for each cluster as well as the percentage of differences with respect to the
314 mean of the overall sampling period in the semi-rural background coastal site as considered affected
315 to regional sources with little contribution from the urban and industrial area. Generally, results
316 show an evident increase of $PM_{2.5}$ and ammonium sulphate when air masses originated from
317 Eastern Europe (+ 40 % and + 124 %, respectively), ammonium nitrate increases when air masses
318 come from Atlantic and Western Mediterranean area (+ 35 % and + 17 %, respectively) and fossil
319 fuel source when air masses blow from South (+ 60 %). On the contrary, industrial, glass making
320 and traffic only slightly increases when masses move from Eastern Europe and in East-Austria.
321 Results also show significant drops of concentrations of $PM_{2.5}$, ammonium nitrate and fossil fuels
322 for Central and Northern Europe clusters.

323
324 Generally, PSCF and CWT analyses return very similar results, but they give some more clues
325 about the potential source location. Resulting PSCF plots for $PM_{2.5}$ and PMF sources are shown in
326 Fig. 2, while their associated uncertainties are provided as Figure SIIa and SIIb. Maps are
327 calculated over the whole sampling campaign and are not smoothed because the low number of
328 trajectories used (only trajectories with concentrations >75th percentile). Uncertainties calculated
329 by bootstrapping the trajectories are generally low for all the variables, allowing to extract the
330 following information. High probabilities (range 0.5-0.6) of high levels of fossil fuels combustion
331 and ammonium nitrate are found in Po Valley, while industrial, ammonium sulphate and road traffic
332 contributions show elevated probabilities in East-Europe (range 0.3 - 0.7) and glass-making source
333 from Eastern and Southeastern Countries. With respect to the glass-making sources, it should be
334 noted that near SRB sampling site, there is a local glass-making industry. Hence, the increase of
335 probability can be due to the mix of local air masses with external air masses and not necessarily
336 only from an external contribution.

337 Although CWT distributes concentration along the trajectories similarly to PSCF, this method has
338 an advantage that it distinguishes major sources from moderate ones by calculating concentration
339 gradients (Hsu et al., 2003). CWT maps presented in Fig. 3a and 3b demonstrates smoothed data
340 split for sampling seasons. The concentration gradients indicate Po Valley and East-Europe as
341 significant contributors of $PM_{2.5}$ and related PMF sources. Seasonally, high external contribution
342 can be observed during spring and winter, reaching $40 \mu g m^{-3}$ and $30 \mu g m^{-3}$ for $PM_{2.5}$ and
343 ammonium nitrate, respectively. In addition, other sources show potential external contribution
344 during summer (fossil fuels combustion and glass-making) and autumn (ammonium sulphate,

345 industrial, road-traffic and glassmaking). In particular, the external contributions of ammonium
346 sulphate from East-Europe reach $14 \mu\text{g m}^{-3}$ during autumn and winter.

347

348 Results of trajectory-based methods are interesting for a number of reasons and may have
349 significant implications for air quality assessment and mitigation measures adopted, or to adopt, in
350 the study area. $\text{PM}_{2.5}$ is a critical pollutant in Venice and in the Northern Italy due to the frequent
351 exceeding of European air quality standards.

352

353 Ammonium nitrate and combustion source is the main contributor of $\text{PM}_{2.5}$ apportioned by the PMF
354 analysis and also has PSCF and CWT maps quite identical to $\text{PM}_{2.5}$ for source locations,
355 probability/concentrations and seasonal trends. Under this scenario, it is evident that it plays a key
356 role in breaching of $\text{PM}_{2.5}$ standards. Although the source apportionment has not separated the two
357 main components behind this source (likely because of the limitation to distinguish elemental and
358 organic carbon), results indicate they have likely a similar potential origin, which is principally
359 linked to weather conditions and anthropogenic emissions. Nitrate aerosol mainly derives from the
360 atmospheric oxidation of NO_2 and the combustion of fossil fuels (road traffic and industries) is by
361 far the dominant source of nitrogen oxides in Europe. Moreover, nitrate is a semi-volatile
362 compound and its partitioning is favoured toward particle-phase in coldest periods. Similarly,
363 combustion emissions generally increase in coldest periods due to contributions from domestic
364 heating and the recent increase of the number of pellet stoves in use in Northern Italy is expected to
365 boost this trend. Results of PSCF and CWT show a strong potential contribution from regional
366 transports from Po Valley (spring, autumn, winter) and from Central (spring) and Eastern (winter)
367 Europe. These findings are in line with the EEA airbase maps (EEA, 2015), which clearly show that
368 Northern Italy, Central Europe and in minor extent some Eastern Countries are affected by the
369 highest annual average levels of measured NO_2 . The seasonal behaviour is also consistent with
370 results, since spring and winter were the coldest periods during the sampling campaign. Moreover,
371 carbonaceous matter that can be considered mainly related to combustion processes presents the
372 highest contribution in central Europe and the ratio TC/PM_{10} is generally larger in this area (Putaud
373 et al., 2010).

374

375 The increasingly high standard for fossil fuels and industrial emissions in Central Europe have lead
376 a significant drop of SO_2 levels in Central and Western Europe to concentrations well below $10 \mu\text{g}$
377 m^{-3} (EEA, 2015). However, SO_2 still reach high concentrations ($>10 \mu\text{g m}^{-3}$) in some Eastern and
378 Southeastern locations (e.g., Poland, Romania, Serbia, Bulgaria, Greece and Turkey). Since SO_2 is
379 the main precursor of sulphate aerosol and ammonium sulphate account for 17 % -24 % of total

380 PM_{2.5} mass in Venice, results of this study indicate a strong influence of trans-boundary transports.
381 However, many studies attribute SO₂ and ammonium sulphate aerosol in the Mediterranean area
382 also to the high maritime traffic in particular for the role of SO₂ as gaseous precursor on secondary
383 formation processes (e.g.: Cesari et al., 2014; Salameh et al., 2015), nevertheless shipping emissions
384 are not the main trigger of PM pollution episodes encountered in the Mediterranean basin (Salameh
385 et al., 2015).

386 Moreover, a recent study conducted in the Veneto region (Masiol et al., 2015) demonstrated that
387 sulphate levels are constant, showing similar daily trends and mean throughout the region and
388 highlighting that both the accumulation/removal processes in the region are similar. In regards to
389 SO₂, Sacca Fisola (a Venice monitoring station close to the Grand Canal where cruise ships pass)
390 shows similar concentration to the IND site on annual mean (ARPAV, 2011). IND site is affected
391 by industrial activities (petrochemical plant, coal power plant) and shipping traffic. Therefore,
392 despite maritime traffic contributes strongly to pollutant source in the coastal area, in the study area
393 it can be considered negligible with respect to other contributions.

394
395 Although glass-making industry source is considered of local origin because the emissions from the
396 Island of Murano, the high probability in PSCF and the high concentration gradient in CWT are not
397 surprising. The trajectories coming from SE are often associated with typical wind regimes called
398 “Scirocco”, which bring hot and wet air masses from the Adriatic region. Under this wind regime,
399 the Island of Murano is just upwind to the sampling sites and the results of trajectory analyses may
400 be subjected to an artefact. However, a transboundary origin cannot be excluded for this source. The
401 elemental tracer in this source (As and Cd) can be also linked to industrial processes, mining and
402 other anthropogenic activities (Moreno et al., 2006; Lim et al., 2010).

403 404 *4.3 Cluster on wind data and CPF*

405 Five groups of days with similar atmospheric circulation patterns were found in data obtained from
406 both the weather stations. A 15 % cut-off level has been applied while processing data. Average
407 wind speeds (Ws) and predominant directions were then plotted for the full period and each group
408 in Fig. 4. Kruskal-Wallis test has been applied to highlight which sources are statistically different
409 (p value < 0.05) respect to the average conditions (all sampled days) among the identified groups.

410
411 Group 1 (N=44) includes days with prevailing wind from quadrant I, with high speeds and very low
412 percentage of calm wind hours (0.5 %). Fast north-easterly winds called “bora” form peculiar cold
413 and gusty downslope windstorms blowing over the Adriatic Sea and bringing air masses from
414 Northern Europe. Generally, in the study area these conditions may cause increased sea-spray

415 generation and dispersion of pollutants (Masiol et al. 2010). In fact, in these conditions, a general
416 decrease of all contributions can be observed in all three sites, in particular for industrial, glass-
417 making and ammonium nitrate show a clear drop in contributions (-54 %, -48 %, -83 % on mean,
418 respectively) and are statistically different to the full period mean. Group 2 (N=93) includes days
419 with middle intensity winds blowing mainly from N-NE, other directions are negligible. This group
420 is mainly composed of autumn and winter days and can represent the atmospheric circulation
421 occurring during cold periods. In these days, fossil fuels contribution decrease and, on the contrary
422 an increase in industrial component can be observed in IND (+39 %) and URB sites (+42 %) as
423 well as traffic (+35 % and +34 % in IND and URB, respectively). This shows that the wind speed is
424 decisive in the dispersion of pollutants and even a small decrease could lead to a widespread
425 accumulation of pollutants.

426 Group 3 (N=75) includes conditions with ~50 % of winds from quadrant I and ~50 % of winds from
427 the quadrant II. Winds from quadrant II are frequent mainly during the warmer seasons, in fact no
428 winter days are included due to the sea-breeze circulation, but they can describe a peculiar wind
429 pattern called “Scirocco,” bringing warm air masses from southern Adriatic and Mediterranean
430 regions. Fossil fuels, industrial and ammonium nitrate are statistically different to the full period
431 mean: fossil fuels shows an increase in contribution (+49% and +21% in IND and URB,
432 respectively) while industrial and ammonium nitrate contributions decrease with the lowest
433 contributions reached in SRB (-51% and -55%, respectively). The highest wind speed (2.0 - 2.7 m s⁻¹)
434 favours the dispersion of these sources but enhance the transport of fossil fuel related compounds.
435 Moreover, the decrease on ammonium nitrate contribution can be also linked to the fact that winter
436 samples (enriched in nitrate and ammonium) are not included in this group.

437 Group 4 includes only spring days (SRB=31; IND=27; URB=29) characterized by wind blowing
438 from SE. In these conditions clean air from Adriatic Sea results in low contributions of all sources
439 except fossil fuels combustion. Similar to group 3, wind from II quadrant enhances the input of
440 fossil component (+44 %, +80 % and +61 % in IND, URB and SRB respectively). Group 5 (N=11)
441 includes days characterized by a high percentage of wind calm (about 20 %), low speeds (1 - 1.9
442 m/s) and no prevailing direction. These “stagnation” conditions were associated to the rise of
443 locally emitted pollutants (Masiol et al., 2010); in fact an increase of industrial and ammonium
444 nitrate contribution can be observed in all three sites (+30 % and +50 % on mean, respectively).
445 Among the identified sources, industrial, ammonium nitrate and fossil fuel combustion appear more
446 sensitive to atmospheric circulation changes. In particular, fossil fuels contribution enhance in days
447 characterized by wind blowing from SE (group 3 and 4) while industrial and ammonium nitrate
448 levels are most affected by the different wind speed. Despite this, our analysis does not help in

449 understanding the source locations with respect to each sampling site, may be due to a widespread
450 pollution condition that affects the study area.

451 In this view, the application of CPF method provides the most probable sources of pollution for
452 each location. CPF values for each sources that apportion to PM_{2.5} are plotted in polar coordinates in
453 Fig. 5. CPF permits to better highlight the possible location of each identified source. The highest
454 probabilities are reached to the sources characterized by a significant local contribution (traffic,
455 industrial and glass-making) whereas the probability associated to ammonium nitrate and
456 ammonium sulphate tends to be lower according to their secondary origin and the homogeneous
457 distribution in the study area (Squizzato et al., 2012).

458 Traffic shows high probability toward east in all three sites and south in URB and IND site in
459 correspondence with the street located near the sampling sites.

460 In SRC the highest probability for industrial contribution is reached toward north: this may be due
461 to the influence of the engineering works for the construction of high-tide preventing dams at the
462 Venice Lagoon entrance.

463 The highest probability for glass-making is reached toward south and east in IND site due to the
464 emissions of local industries in Murano Island, located east of the site. Fossil fuels shows the
465 highest probability associated to wind blowing from SE. This highlights the influence of the
466 combustion processes occurring in the industrial zone on URB and IND site. In regards to SRB site,
467 the increase of probability can be due to the ship traffic toward Venice.

468

469 *4.5 Lenschow approach*

470 Yearly, local sources contribute for 9.8 $\mu\text{g m}^{-3}$ of PM_{2.5} amounting to 28 % and 30 % of masses in
471 URB and IND site respectively (Table 2). Seasonally, the highest local contributions were observed
472 in spring and winter both in URB (11.3 $\mu\text{g m}^{-3}$ and 15.5 $\mu\text{g m}^{-3}$) and IND site (10.4 $\mu\text{g m}^{-3}$ and
473 12.5 $\mu\text{g m}^{-3}$) whereas the highest percentage was reached in summer (31 % in URB and 40.5 % in
474 IND site). Among the identified sources, ammonium nitrate and ammonium sulphate show the
475 lowest local contribution (31 % and 26 % respectively) confirming the results obtained applying the
476 CWT, highlighting high external contribution for these sources. Traffic sources show the highest
477 local contribution (83 % and 74 % in URB and IND site respectively), followed by glass making,
478 industrial and fossil fuels combustion.

479 During heavy PM events (> 75th percentile) local contribution on PM expressed in $\mu\text{g m}^{-3}$ increases
480 (20.4 $\mu\text{g m}^{-3}$) whereas the local contribution percentages are similar to the average conditions (28.4
481 % and 27.7 %, respectively). Nevertheless, considering the mass percentage, no significant
482 variations have been observed for all periods and samples for PM and its sources. Fossil fuels

483 source represents an exception: during these events the local contribution reaches the 56 % and the
484 63 % in URB and IND respectively that is about twice the average percentage of samples.
485 On this basis, local contribution is important and it is strongly affected to local atmospheric
486 circulation that governs the level of PM and its component. During high polluted episodes the local
487 contributions do not increase and the increase of PM and related sources can be addresses to
488 external contribution.

489

490 **Conclusions**

491 The knowledge of ground-wind circulation and potential long-range transports is fundamental to
492 evaluate how and how much local or external sources may affect the air quality at a receptor site.
493 In this study, the results of a recent source apportionment study carried out in Venice (Eastern Po
494 Valley) are used as input for different statistical approaches. Meteorology-based methods (back-
495 trajectories and wind-based methods) have been used to determine the influence of external and
496 local contribution on identified PM_{2.5} sources.

497 About applied methodologies some consideration can be done:

- 498 • Cluster on back-trajectories represents an easy but effective method to evaluate the potential
499 effects of long-range/regional transports. It helps in understanding the area of origin but
500 does not provide a precise location.
- 501 • Generally, PSCF and CWT analyses return very similar results to cluster but they give some
502 more clues about the potential source location.
- 503 • Despite CWT distributes concentration along the trajectories similarly to PSCF, this method
504 has an advantage: it distinguishes major sources from moderate ones by calculating
505 concentration gradients and it becomes more effective in estimating of external
506 contributions.
- 507 • Cluster on wind data partially help in understanding the source locations respect to each
508 sampling site. The analysis can be affected to widespread pollution condition and the wind
509 speed component tends to dominates in the interpretations of results respect to direction.
- 510 • The application of CPF provides understanding of the most probable sources location, with
511 the highest probability associated to the local sources respect to the external ones (e.g. road
512 traffic).
- 513 • Lenschow's approach represents a useful method to estimate local contribution but it
514 requires to have a good knowledge of the study area and its emission sources and more than
515 one measurement sites at least one of these considerable as a background site. This may be a
516 limitation to its applicability.

517 Obtained results highlighted the complexity of atmospheric dynamics in the study area and our
518 influence on PM and sources levels: (i) external contributions are a not negligible intake of PM_{2.5}
519 and (ii) local atmospheric circulation determines different levels of source contribution and some
520 specific direction have been detected.

521 PM sources contributions are influenced by external contribution coming mainly from Po Valley
522 and East-Europe. Seasonally, high external contribution can be observed during spring and winter
523 reaching 40 $\mu\text{g m}^{-3}$ and 30 $\mu\text{g m}^{-3}$ for PM_{2.5} and ammonium nitrate, respectively. Moreover, the
524 external contributions of ammonium sulphate, that represent the second PM mass source, reach 14
525 $\mu\text{g m}^{-3}$ during autumn and winter over East-Europe.

526 Among the identified sources, industrial, ammonium nitrate and fossil fuel combustion appear more
527 sensitive to local atmospheric circulation changes. In particular, fossil fuels contribution enhance in
528 days characterized by wind blowing from SE while industrial and ammonium nitrate levels are most
529 affected by the different wind speed. Other sources do not show a strong dependence on the wind
530 direction.

531 Lenschow's approach has allowed to estimate the local contribution on PM and its sources: yearly,
532 local sources contribute for 9.8 $\mu\text{g m}^{-3}$ of PM_{2.5} amounting to 28 % and 30 % of masses in URB and
533 IND site, respectively. During heavy PM events the local contribution percentage are similar to the
534 average conditions (28.4 % and 27.7 %, respectively), hence the increase of PM and related sources
535 can be mainly addresses to external contribution. Only fossil fuels represent an exception: during
536 these events the local contribution reaches the 56 % and the 63 % in URB and IND, respectively,
537 about twice the average percentage of samples.

538

539 **Acknowledgment**

540 The authors would like to thanks Ente Zona Industriale di Porto Marghera (<http://www.entezona.it/>)
541 for the financial support to the project "Study of secondary particulate matter in the Venice area",
542 ARPAV and Comando Zona Fari e Segnalamenti Marittimi di Venezia for logistics.

543 The authors gratefully acknowledge the NOAA Air Resources Laboratory (ARL) for providing the
544 HYSPLIT transport and dispersion model and access to READY website
545 (<http://ready.arl.noaa.gov>).

546

547 **REFERENCES**

548 Ashbaugh, L. L., Malm, W. C., and Sadeh, W. Z., 1985. A Residence Time Probability Analysis of
549 Sulfur Concentrations at Ground Canyon National Park. *Atmos. Environ.* 19(8), 1263–1270.

550 ARPAV, 2011. Air quality in Venice, Annual report 2010. In Italian, available at:

551 <http://www.arpa.veneto.it/arpav/chi-e-arpav/file-e-allegati/dap-venezia/aria/RQA2010.pdf>.

- 552 Brereton, C.A., Johnson, M.R., 2012. Identifying sources of fugitive emissions in industrial
553 facilities using trajectory statistical methods. *Atmos. Environ.* 51, 46–55.
- 554 Carslaw D.C., Beevers S.D., Ropkins K., Bell M.C., 2006. Detecting and quantifying aircraft and
555 other on-airport contributions to ambient nitrogen oxides in the vicinity of a large
556 international airport. *Atmos. Environ.* 40, 5424–5434.
- 557 CEN (Comité Européen de Normalisation), 2005. Ambient air quality — standard gravimetric
558 measurements for the determination of the PM_{2.5} mass fraction of suspended particulate
559 matter. EN 14907:2005.
- 560 Cesari D., Genga, A., Ielpo, P., Siciliano, M., Mascolo, G., Grasso, F. M., Contini, D., 2014. Source
561 apportionment of PM_{2.5} in the harbour–industrial area of Brindisi (Italy): Identification and
562 estimation of the contribution of in-port ship emissions. *Sci. Total Environ.* 497–498, 392–
563 400.
- 564 Cheng, I., Zhang, P., Blanchard, P., Dalziel, J., Tordon, R., 2013. Concentration-weighted trajectory
565 approach to identifying potential sources of speciated atmospheric mercury at an urban
566 coastal site in Nova Scotia, Canada. *Atmos. Chem. Phys.* 13, 6031–6048.
- 567 Darby, L., 2005. Cluster analysis of surface winds in Houston, Texas, and the impact of wind
568 patterns on ozone. *J. Appl. Meteorol.* 44, 1788–1806.
- 569 Draxler R.R., Rolph G.D., 2015. HYSPLIT (HYbrid Single-Particle Lagrangian Integrated
570 Trajectory) Model access via NOAA ARL READY Website
571 (<http://www.arl.noaa.gov/HYSPLIT.php>). NOAA Air Resources Laboratory, College Park,
572 MD.
- 573 Dvorska, A., Lammel, G., Klanova, J., Holoubek, I., 2008. Kosetice, Czech Republic – ten years of
574 air pollution monitoring and four years of evaluating the origin of persistent organic
575 pollutants. *Environ. Pollut.* 156, 403–408.
- 576 EEA (European Environment Agency), 2015. AirBasedThe European Air Quality Database.
577 Available from: <http://www.eea.europa.eu/themes/air/air-quality/map/airbase> (last accessed
578 February, 2015).
- 579 Fleming Z.L., Monks P.S., Manning A.J., 2012. Review: Untangling the influence of air-mass
580 history in interpreting observed atmospheric composition. *Atmos. Res.* 104-105, 1–39.
- 581 Gilardoni, S., Vignati, E., Cavalli, F., Putaud, J. P., Larsen, B. R., Karl, M., Stenström, K., Genberg,
582 J., Henne, S., 2011. Better constraints on sources of carbonaceous aerosols using a combined
583 ¹⁴C – macro tracer analysis in a European rural background site. *Atmos. Chem. Phys.* 11,
584 5685–5700.
- 585 Gildemeister, A. E., Hopke, P. K., Kim, E., 2007. Sources of fine urban particulate matter in
586 Detroit, MI. *Chemosphere* 69, 1064–1074.
- 587 Han, Y.-J., Holsen, T. M., and Hopke, P. K., 2007. Estimation of source locations of total gaseous
588 mercury measured in New York State using trajectory-based models. *Atmos. Environ.* 41,
589 6033–6047.

- 590 Hopke, P.K., Li, C.L., Ciszek, W., Landsberger, S., 1995. The use of bootstrapping to estimate
591 conditional probability fields for source locations of airborne pollutants. *Chemometr. Intell.*
592 *Lab.* 30, 69-79.
- 593 Hsu, Y., Holsen, T.M., Hopke, P.K., 2003. Comparison of hybrid receptor models to locate PCB
594 sources in Chicago. *Atmos. Environ.* 37, 545–562.
- 595 Kabashnikov, V. P., Chaikovsky, A. P., Kucsera, T. L., and Metelskaya, N. S., 2011. Estimated
596 accuracy of three common trajectory statistical methods. *Atmos. Environ.* 45, 5425–5430.
- 597 Kaufmann, P., Whiteman, C.D., 1999. Cluster-analysis classification of wintertime wind patterns in
598 the Grand Canyon region. *J. Appl. Meteorol.* 38, 1131–1147.
- 599 Kim, E., Hopke, P.K., Edgerton, E.S., 2003. Source Identification of Atlanta Aerosol by Positive
600 Matrix Factorization. *J. Air Waste Manage. Assoc.* 53, 731–739.
- 601 Kim, E., Hopke, P. K., 2004. Comparison between Conditional Probability Function and
602 Nonparametric Regression for Fine Particle Source Directions. *Atmos. Environ.* 38, 4667 –
603 4673.
- 604 Kim, E., Hopke, P.K., Kenski, D.M., Koerber, M., 2005. Sources of Fine Particles in a Rural
605 Midwestern U.S. Area. *Environ. Sci. Technol.* 39, 4953–4960.
- 606 Kundu S., Kawamura, K., Andreae TW., Hoffer A., Andreae M.O., 2010. Diurnal variation in the
607 water-soluble inorganic ions, organic carbon and isotopic compositions of total carbon and
608 nitrogen in biomass burning aerosols from the LBA-SMOCC campaign in Rondônia, Brazil.
609 *J. Aerosol Sci.* 41, 118–133.
- 610 Larsen, B. R., Gilardoni, S., Stenström, K., Niedzialek, J., Jimenez, J., Belis, C. A., 2012. Sources
611 for PM air pollution in the Po Plain, Italy: II. Probabilistic uncertainty characterization and
612 sensitivity analysis of secondary and primary sources. *Atmos. Environ.* 50, 203–213.
- 613 Lee, J.H., Hopke, P.K., 2006. Apportioning sources of PM_{2.5} in St. Louis, MO using speciation
614 trends network data. *Atmos. Environ.* 40, 360–377.
- 615 Lenschow, P., Abraham, H.-J., Kutzner, K., Lutz, M., Preuß, J.-D., Reichenbacher, W., 2001. Some
616 ideas about the sources of PM₁₀. *Atmos. Environ.* 35, S23–S33.
- 617 Lim, J.-M., Lee, J.-H., Moon, J.-H., Chung, Y.-S., Kim, K.-H., 2010. Airborne PM₁₀ and metals
618 from multifarious sources in an industrial complex area. *Atmos. Res.* 96, 53–64.
- 619 Lupu, A., Maenhaut, W., 2002. Application and comparison of two statistical trajectory techniques
620 for identification of source regions of atmospheric aerosol species. *Atmos. Environ.* 36, 5607–
621 5618.
- 622 Masiol, M., Rampazzo, G., Ceccato, D., Squizzato, S., Pavoni B., 2010. Characterization of PM₁₀
623 sources in a coastal area near Venice (Italy): An application of factor-cluster analysis.
624 *Chemosphere* 80, 771–778.
- 625 Masiol M., Squizzato S., Ceccato D., Rampazzo G., Pavoni B., 2012a. Determining the influence of
626 different atmospheric circulation patterns on PM₁₀ chemical composition in a source
627 apportionment study. *Atmos. Environ.* 63, 117-124.
- 628 Masiol, M., Centanni, E., Squizzato, S., Hofer, A., Pecorari, E., Rampazzo, G., Pavoni, B., 2012b.
629 GC-MS analyses and chemometric processing to discriminate the local and long-distance

- 630 sources of PAHs associated to atmospheric PM_{2.5}. *Environ. Sci. Pollut. Res.* 19 (8), 3142-
631 3151.
- 632 Masiol, M., Squizzato, S., Rampazzo, G., Pavoni, B., 2014b. Source apportionment of PM_{2.5} at
633 multiple sites in Venice (Italy): Spatial variability and the role of weather. *Atmos. Environ.*
634 98, 78–88.
- 635 Masiol M., Benetello F., Harrison R.M., Formenton G., De Gaspari F., Pavoni B., 2015. Spatial,
636 seasonal trends and transboundary transport of PM_{2.5} inorganic ions in the Veneto Region
637 (Northeast Italy). *Atmos. Environ.* 117, 19–31.
- 638 Maurizi, A., Russo, F., Tampieri, F., 2013. Local vs. external contribution to the budget of
639 pollutants in the Po Valley (Italy) hot spot. *Sci. Total Environ.* 458–460, 459–465.
- 640 Moreno, T., Querol, X., Alastuey, A., Viana, M., Salvador, P., Sanchez de la Campa, A., Artiñano,
641 B., de la Rosa J., Gibbons, W., 2006. Variation in atmospheric PM trace metal content in
642 Spanish towns: illustrating the chemical complexity of the inorganic urban aerosol cocktail.
643 *Atmos. Environ.* 40, 6791–6803.
- 644 Pekney, N. J., Davidson, C. I., Zhou, L., Hopke, P. K., 2006. Application of PSCF and CPF to
645 PMF-Modeled Sources of PM_{2.5} in Pittsburgh. *Aerosol Sci. Technol.* 40, 952–961.
- 646 Putaud, J.-P., Van Dingenen, R., Alastuey, A., Bauer, H., Birmili, W., Cyrys, J., Flentje, H., Fuzzi,
647 S., Gehrig, R., Hansson, H.C., Harrison, R.M., Herrmann, H., Hitenberger, R., Hüglin, C.,
648 Jones, A.M., Kasper-Giebl, A., Kiss, G., Kousa, A., Kuhlbusch, T.A.J., Löschan, G.,
649 Maenhaut, W., Molnar, A., Moreno, T., Pekkanen, J., Perrino, C., Pitz, M., Puxbaum, H.,
650 Querol, X., Rodriguez, S., Salma, I., Schwarz, J., Smolik, J., Schneider, J., Spindler, G., ten
651 Brink, H., Tursic, J., Viana, M., Wiedensohler, A., Raes, F., 2010. A European aerosol
652 phenomenology – 3: Physical and chemical characteristics of particulate matter from 60 rural,
653 urban, and kerbside sites across Europe. *Atmos. Environ.* 44, 1308–1320.
- 654 Rolph, G.D., 2015. Real-time Environmental Applications and Display sYstem (READY) Website
655 (<http://www.ready.noaa.gov>). NOAA Air Resources Laboratory, College Park, MD.
- 656 Rutter, A. P., Snyder, D. C., Stone, E. A., Schauer, J. J., Gonzalez-Abraham, R., Molina, L. T.,
657 Márquez, C., Cárdenas, B., and de Foy, B., 2009. In situ measurements of speciated
658 atmospheric mercury and the identification of source regions in the Mexico City Metropolitan
659 Area. *Atmos. Chem. Phys.* 9, 207–220.
- 660 Salameh, D., Detournay, A, Pey, J., Pérez, N., Liguori, F., Saraga, D., Bove, M. C., Brotto, P.,
661 Cassola, F., Massabò, D., Latella, A., Pillon, S., Formenton, G., Patti, S., Armengaud, A.,
662 Piga, D., Jaffrezò, J., Bartzis, J., Tolis, E., Prati, P., Querol, X., Wortham, H., Marchand, N.,
663 2015. PM_{2.5} chemical composition in five European Mediterranean cities: A 1-year study.
664 *Atmos. Res.* 155, 102–117.
- 665 Seibert, P., Kromp-Kolb, H., Baltensperger, U., Jost, D.T., Schwikowski, M., Kasper, A., Puxbaum,
666 H., 1994. Trajectory analysis of aerosol measurements at high alpine sites. In: Borrell, P.M.,
667 Borrell, P., Cvitas, T., Seiler, W. (Eds.), *Transport and Transformation of Pollutants in the*
668 *Troposphere*, Academic Publishing, Den Haag (1994), pp. 689–693.

- 669 Squizzato, S., Masiol, M., Innocente, E., Pecorari, E., Rampazzo, G., Pavoni, B., 2012. A procedure
670 to assess local and long-range transport contributions to PM_{2.5} and secondary inorganic
671 aerosol. *J. Aerosol Sci.* 46, 64-76.
- 672 Squizzato, S., Masiol, M., Visin, F., Canal, A., Rampazzo, G., Pavoni, B., 2014. PM_{2.5} chemical
673 composition in an industrial zone included in a large urban settlement: main sources and local
674 background. *Environ. Sci. Proc. Impacts* 16(8), 1913-1922.
- 675 Spencer M.T., Shields L.G., Sodeman D.A., Toner S.M., Prather K.A., 2006. Comparison of oil and
676 fuel particle chemical signatures with particle emissions from heavy and light duty vehicles.
677 *Atmos. Environ.* 40, 5224–5235
- 678 Stohl, A., 1998. Computation, accuracy and applications of trajectories- review and bibliography.
679 *Atmos. Environ.* 32, 947-966.
- 680 Uria-Tellaetxe I., Carslaw D.C., 2014. Conditional bivariate probability function for source
681 identification. *Environ. Model. Softw.* 59 1-9.
- 682 Viana M., Querol X., Alastuey A., Gil J.I., Menéndez M., 2006. Identification of PM sources by
683 principal component analysis (PCA) coupled with wind direction data. *Chemosphere* 65,
684 2411–2418.
- 685 Wehrens, R., Putter, H., Buydens, L.M.C., 2000. The bootstrap: a tutorial. *Chemometr. Intell. Lab*
686 54, 35–52.
- 687 Weiss-Penzias, P. S., Gustin, M. S., and Lyman, S. N., 2011. Sources of gaseous oxidized mercury
688 and mercury dry deposition at two southeastern U.S. sites. *Atmos. Environ.* 45, 4569–4579.

690 **Table captions**

691
692 **Table 1. Average concentrations ($\mu\text{g m}^{-3}$) and percentage difference respect to all samples mean ($\Delta\%$)**
693 **in SRB samples of PM_{2.5} and source contributions for each identified back-trajectories cluster.**

694 **Table 2. Local contribution expressed in $\mu\text{g m}^{-3}$ and % estimated using Lenschow' approach for URB**
695 **and IND site.**

696 **Figure captions**

697
698 **Fig. 1. Sampling site locations (a), gridded back trajectory frequencies (b) and back-**
699 **trajectories clusters (c).**

700 **Fig. 2. PSCF probabilities for PM_{2.5} and identified sources (75th percentile).**

701 **Fig. 3a. CWT for PM_{2.5}, ammonium nitrate and ammonium sulphate sources.**

702 **Fig. 3b. CWT for industrial, traffic, glassmaking and fossil fuel combustion sources.**

703 **Fig. 4. Results of cluster analysis on wind data: box-plots and wind roses for each identified**
704 **cluster (Chs = wind calm hours; Ws = average wind speed). Boxes represent inter-quartile**

705 ranges; squared dots are the median, while whiskers represent quartiles \pm (1.5*inter-quartile
706 ranges).

707 **Fig. 5. CPF plots for the highest 25% of the mass contributions.**

708

709

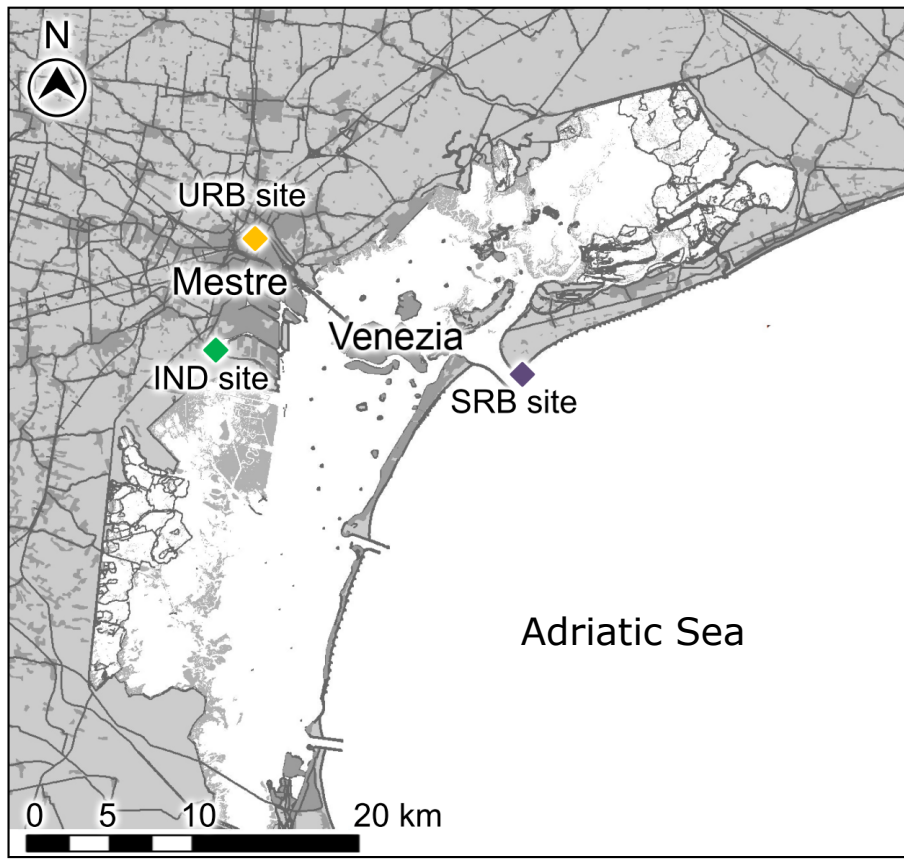
ACCEPTED MANUSCRIPT

Table 1. Average concentrations ($\mu\text{g m}^{-3}$) and percentage difference respect to all samples mean ($\Delta\%$) in SRB samples of $\text{PM}_{2.5}$ and source contributions for each identified back-trajectories cluster.

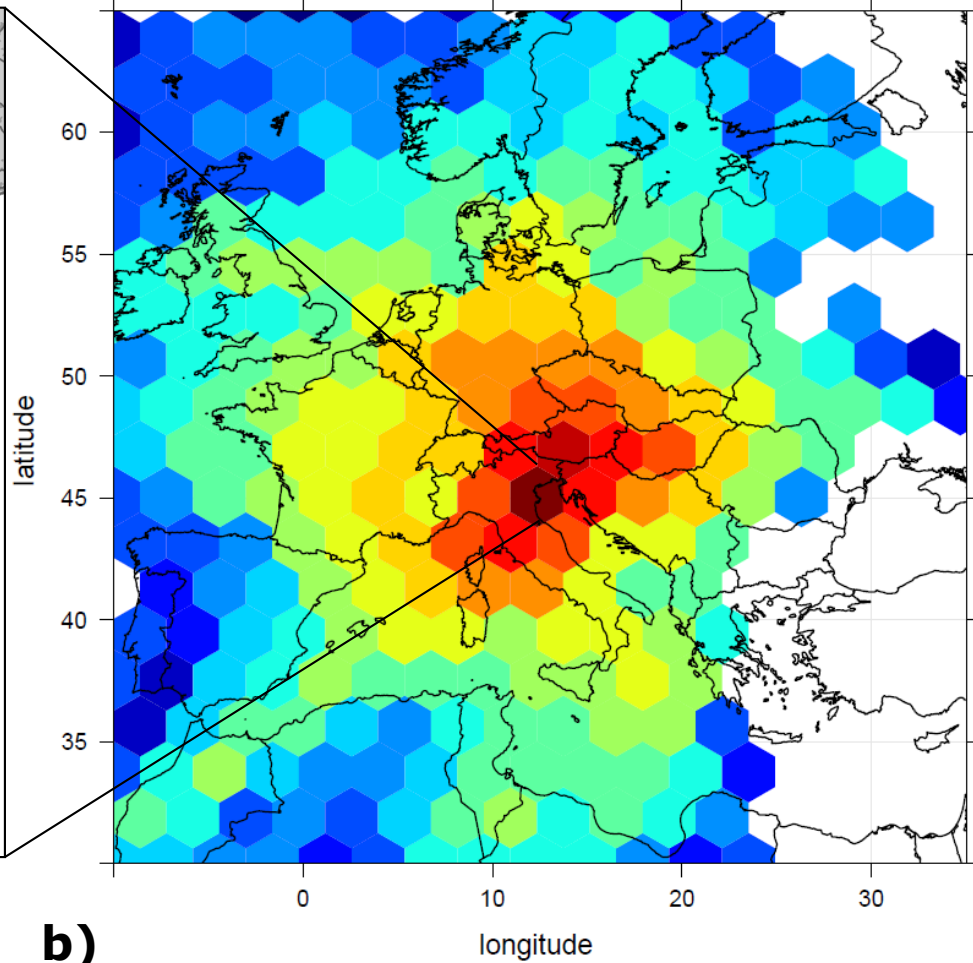
	$\text{PM}_{2.5}$		Industrial		Fossil fuels		Amm. Nitrate		Glass-making		Amm. Sulfate		Road traffic	
	Mean	Δ (%)	Mean	Δ (%)	Mean	Δ (%)	Mean	Δ (%)	Mean	Δ (%)	Mean	Δ (%)	Mean	Δ (%)
Atlantic (N=7)	23.6	-5	3.1	-13	2.2	15	15.8	35	1.6	57	1.0	-83	0.2	-75
Central EU (N=18)	16.2	-35	2.9	-21	2.1	11	7.8	-33	0.7	-30	2.2	-62	0.6	-16
Northern EU (N=14)	15.6	-37	2.4	-34	1.1	-45	9.0	-24	0.8	-27	2.0	-66	0.4	-32
East – Austria (N=42)	26.4	7	4.5	24	1.7	-10	12.0	2	1.4	33	6.1	2	0.9	35
Eastern EU (N=21)	34.6	40	5.8	62	0.9	-54	12.5	7	1.2	18	13.4	124	0.9	39
South (N=37)	25.0	1	2.3	-36	3.1	60	12.3	5	0.8	-26	6.3	5	0.5	-23
Western MED (N=15)	24.9	1	3.4	-5	1.5	-24	13.7	17	0.8	-21	5.1	-14	0.6	-11
All samples	24.7		3.6		1.9		11.7		1.0		6.0		0.7	

Table 2. Local contribution expressed in $\mu\text{g m}^{-3}$ and % estimated using Lenschow' approach for URB and IND site.

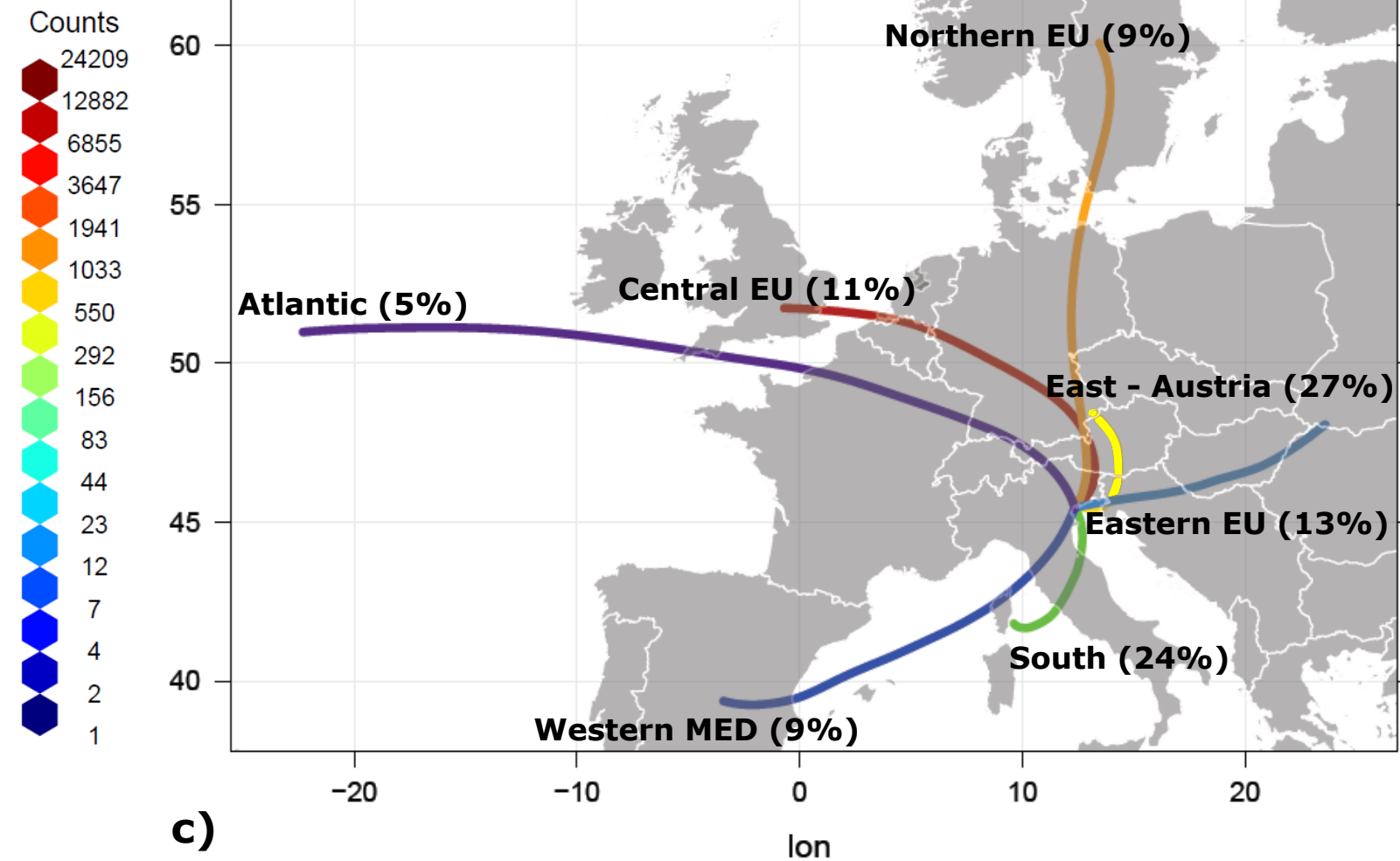
	PM _{local}		Industrial _{local}		Fossil _{local}		Amm. nitrate _{local}		Glass _{local}		Amm. sulfate _{local}		Traffic _{local}	
	$\mu\text{g m}^{-3}$	%	$\mu\text{g m}^{-3}$	%	$\mu\text{g m}^{-3}$	%	$\mu\text{g m}^{-3}$	%	$\mu\text{g m}^{-3}$	%	$\mu\text{g m}^{-3}$	%	$\mu\text{g m}^{-3}$	%
Via Lissa (URB)														
All samples	9.8	27.7	2.5	40.0	1.3	34.8	5.6	31.0	1.2	58.8	1.0	25.6	5.2	82.8
Spring	11.3	26.3	2.5	52.2	1.2	32.0	6.2	20.5	1.6	67.7	1.8	39.0	5.0	86.9
Summer	4.5	31.2	1.7	32.5	1.4	32.2	0.8		1.2	59.3	0.5	20.1	2.5	76.3
Autumn	5.7	24.5	1.6	42.9	1.6	43.2	4.5	50.3	1.1	64.3	0.7	23.9	6.9	84.7
Winter	15.5	28.6	3.3	31.8	0.2	42.5	5.9	30.1	1.1	44.4	1.2	25.7	5.1	81.2
Heavy PM Events (>75 th percentile)	20.4	28.4	4.4	41.8	2.5	56.3	7.9	24.6	1.3	51.7	1.8	19.1	6.1	80.9
Malcontenta (IND)														
All samples	9.8	29.9	4.6	53.8	1.9	54.6	5.1	34.0	1.1	57.5	1.3	31.3	3.4	74.3
Spring	10.4	31.7	4.9	69.3	2.0	46.1	6.3	36.7	1.4	69.5	1.8	42.8	5.1	91.3
Summer	8.9	40.5	3.7	52.8	1.9	40.0	3.6	55.2	1.3	67.3	0.5	28.3	0.6	58.5
Autumn	6.6	25.4	3.1	48.2	2.3	64.4	2.3	39.9	0.5	44.0	1.5	33.0	3.5	75.2
Winter	12.5	24.8	5.9	48.4	1.1	81.9	5.6	28.2	0.8	38.0	1.4	26.6	2.9	66.9
Heavy PM Events (>75 th percentile)	17.6	27.2	6.9	46.0	1.8	62.6	6.0	26.4	0.9	41.8	1.5	20.8	3.6	66.4



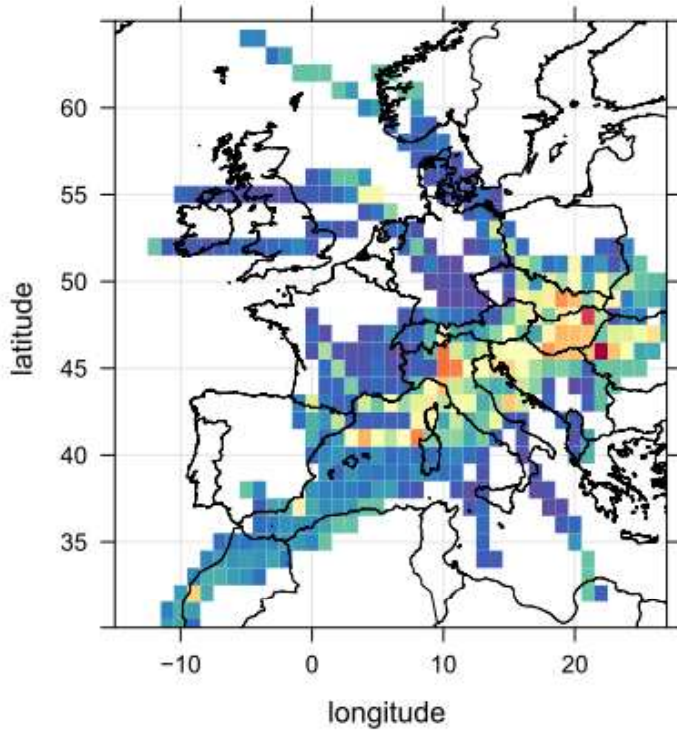
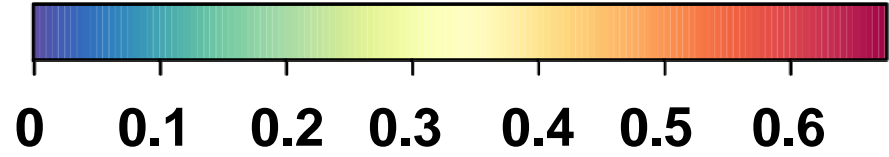
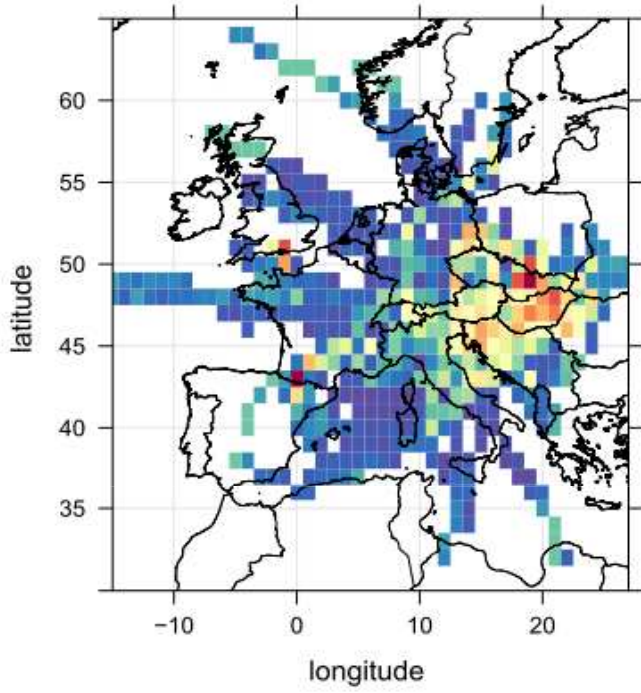
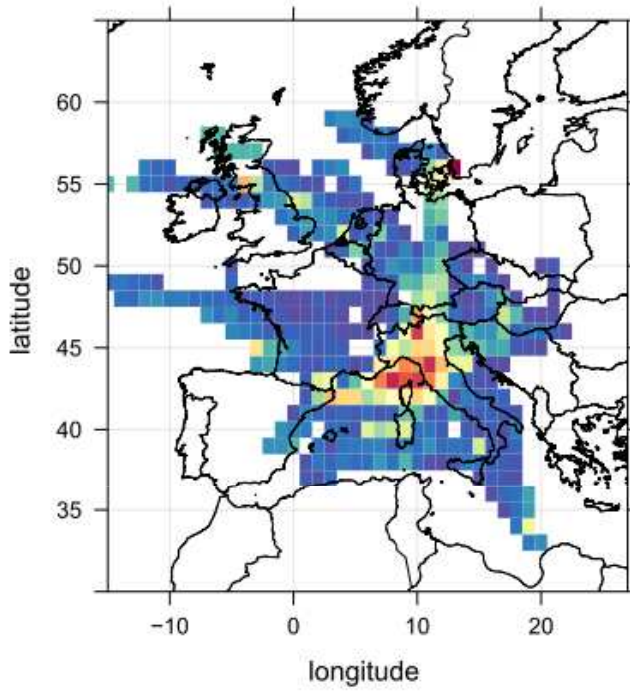
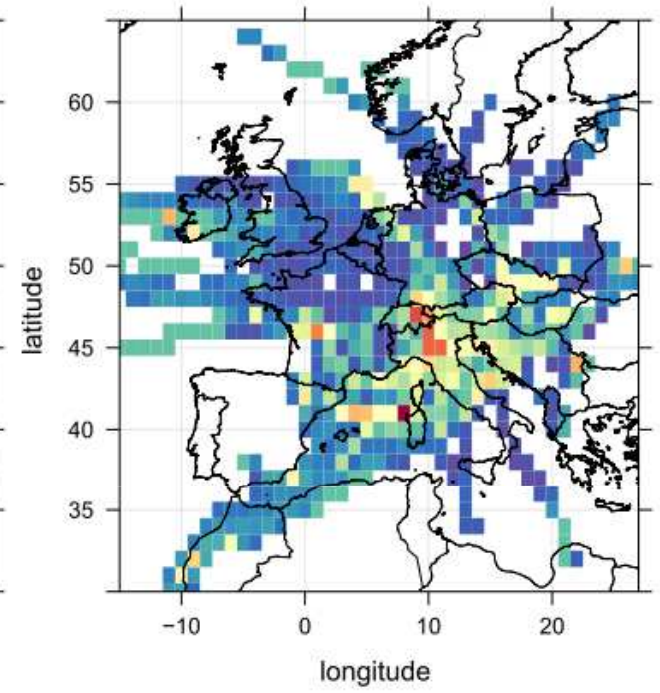
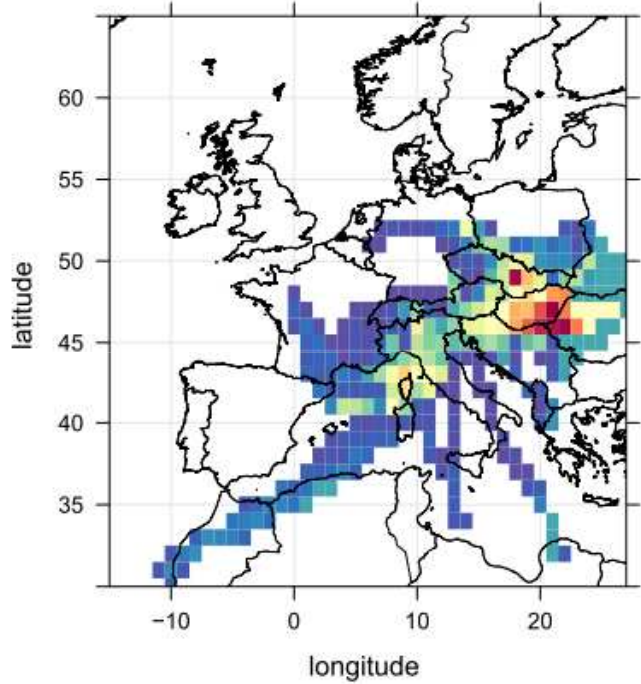
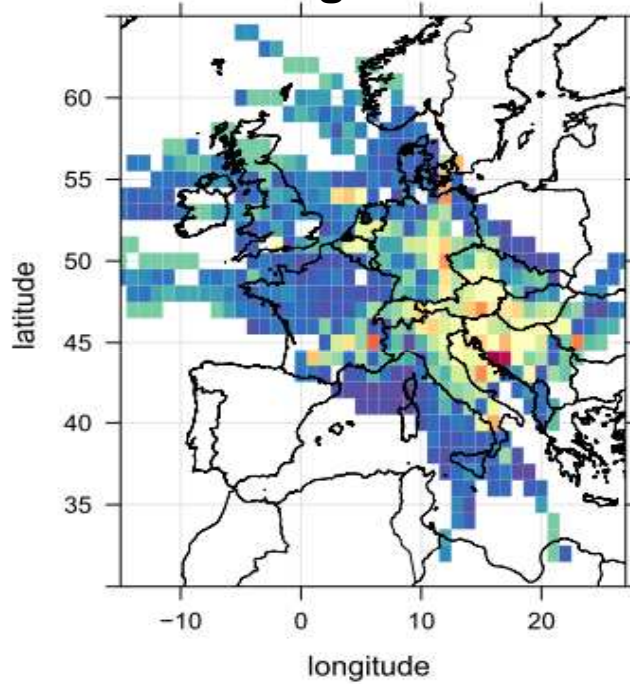
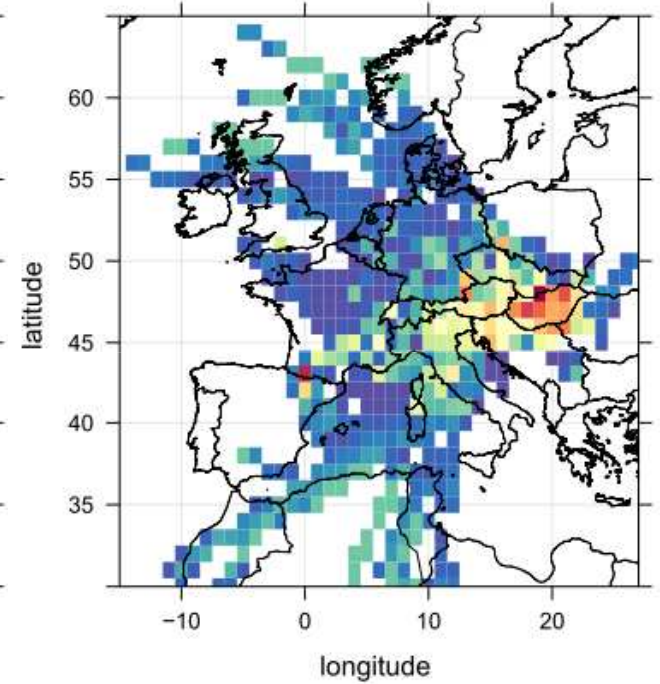
a)

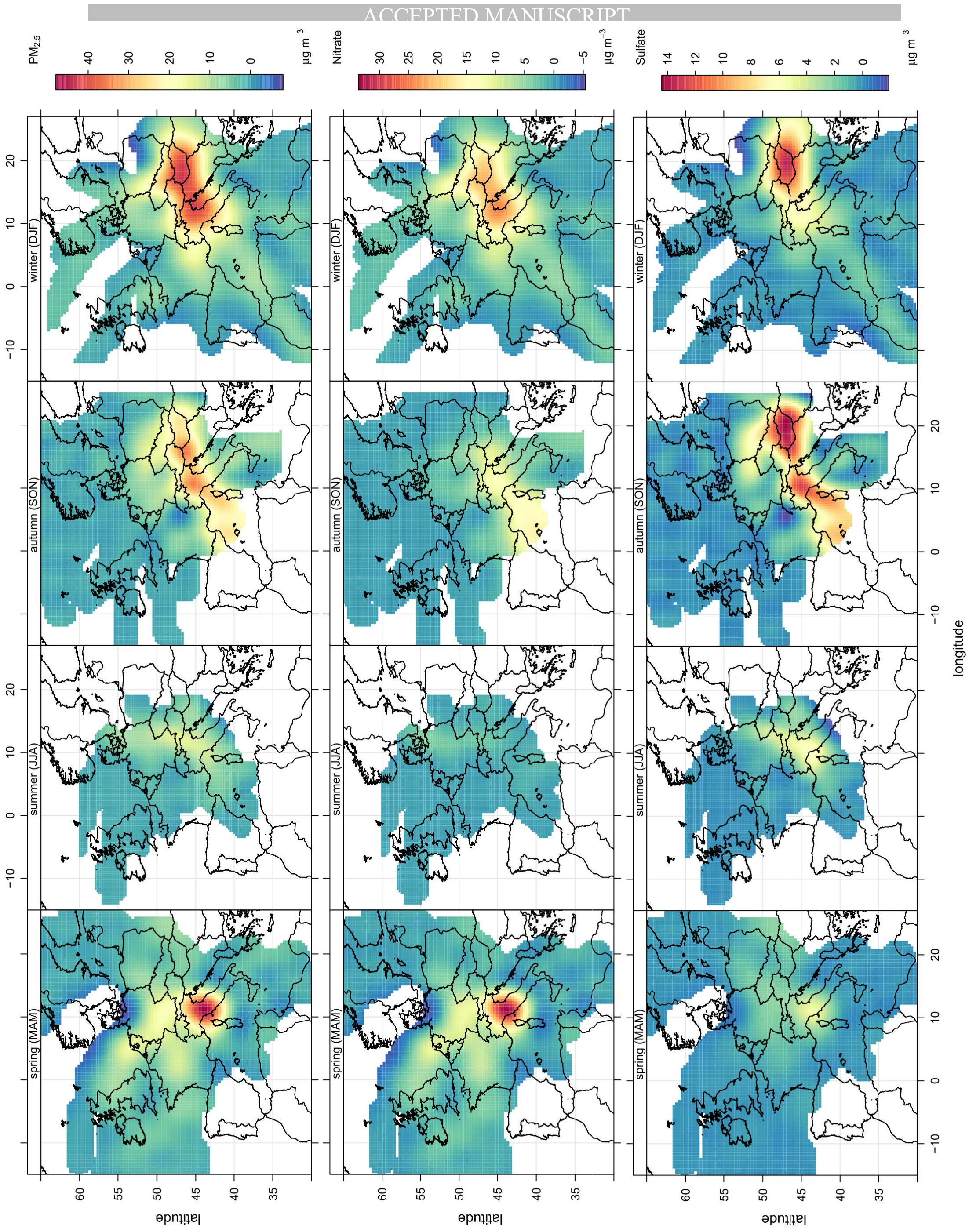


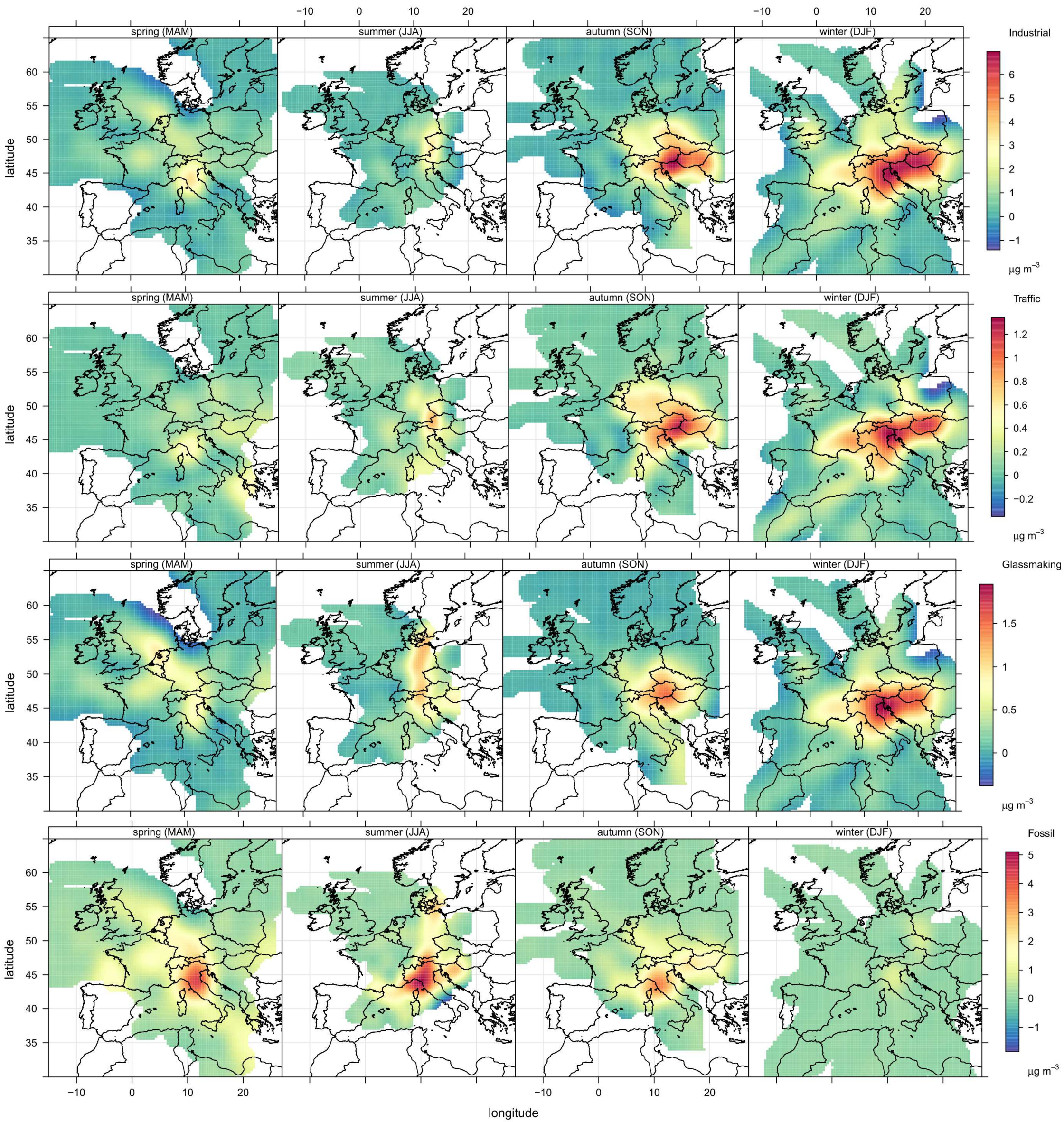
b)



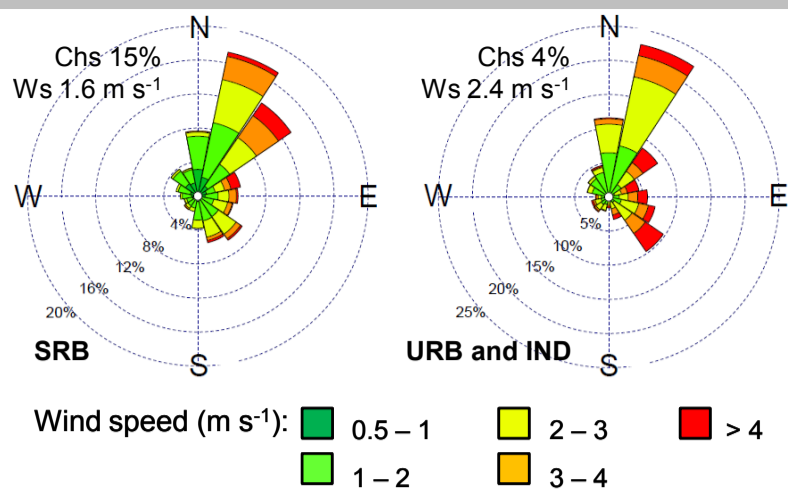
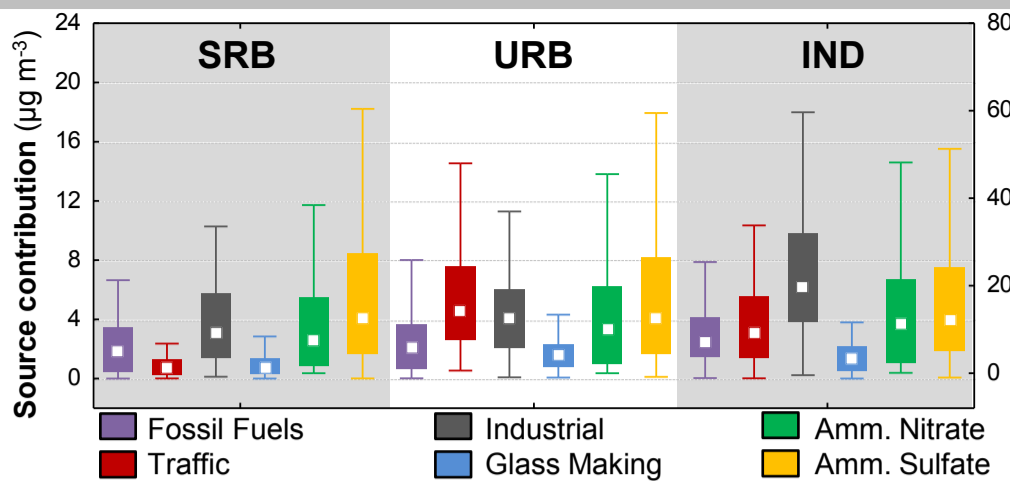
c)

PM_{2.5}**PSCF probability****Industrial****Fossil fuels****Ammonium nitrate****Ammonium sulfate****Glass-making****Traffic**

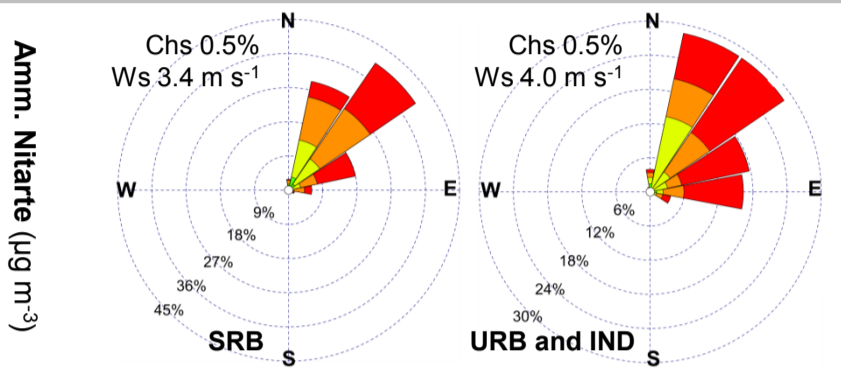
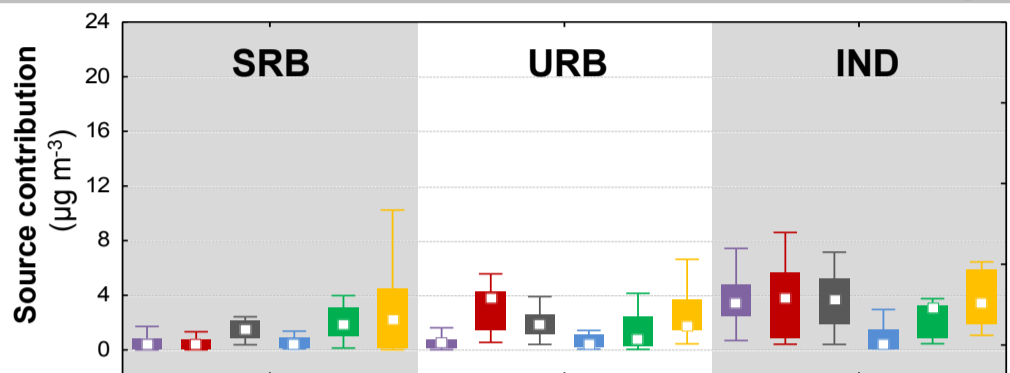




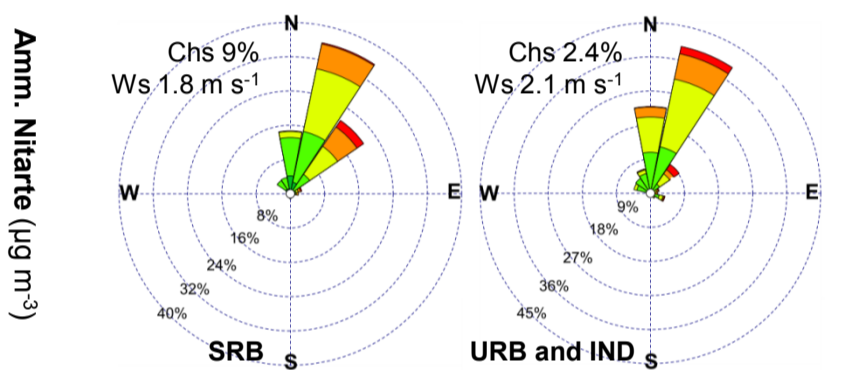
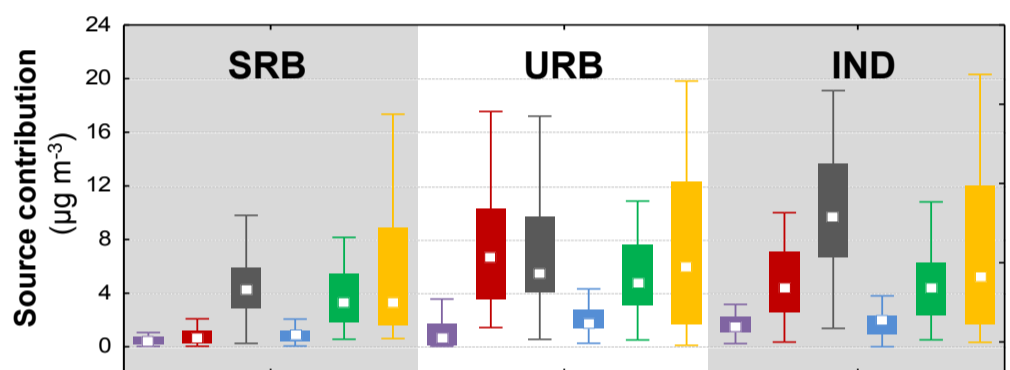
ALL: full period



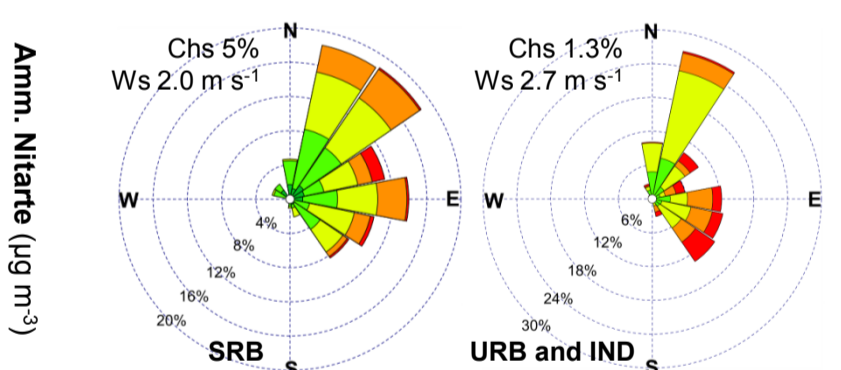
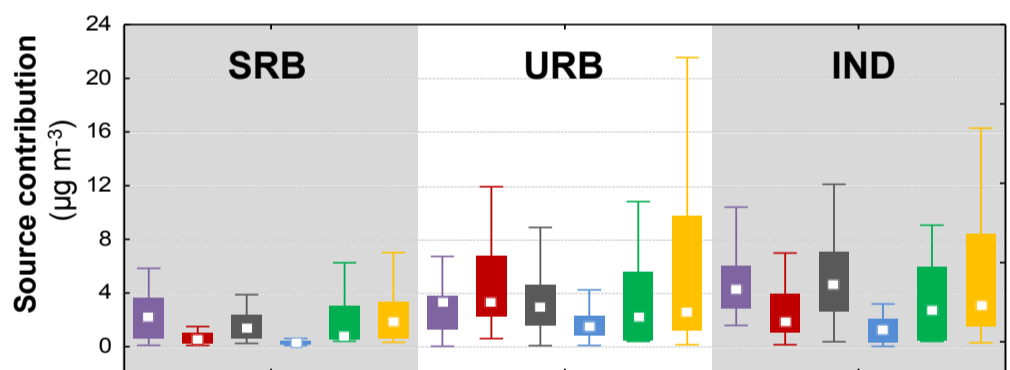
Group 1



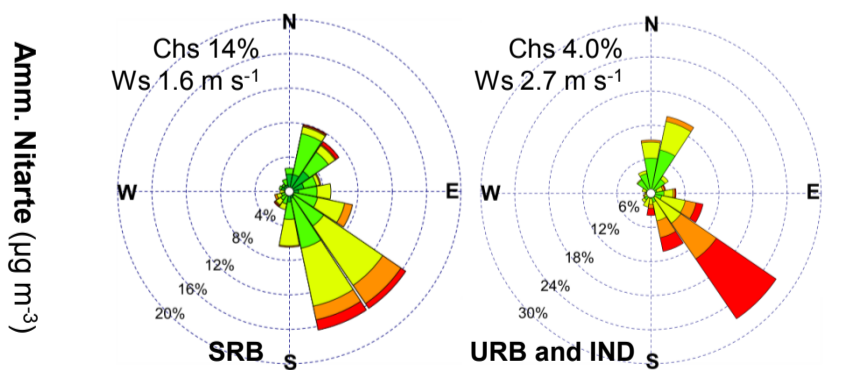
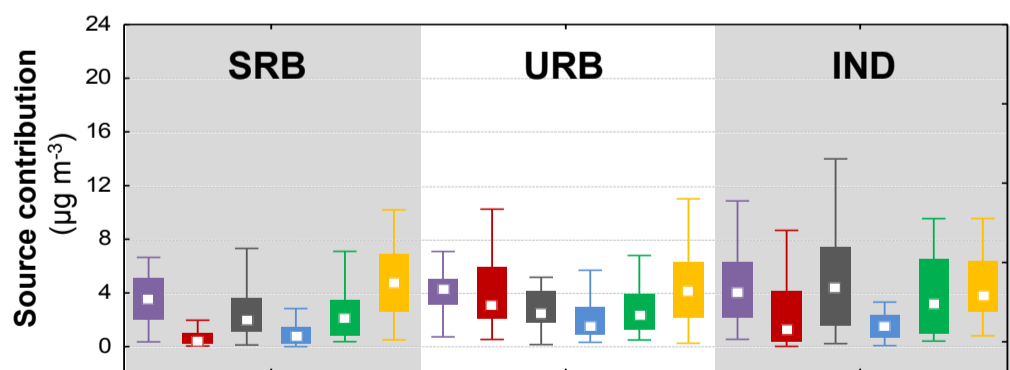
Group 2



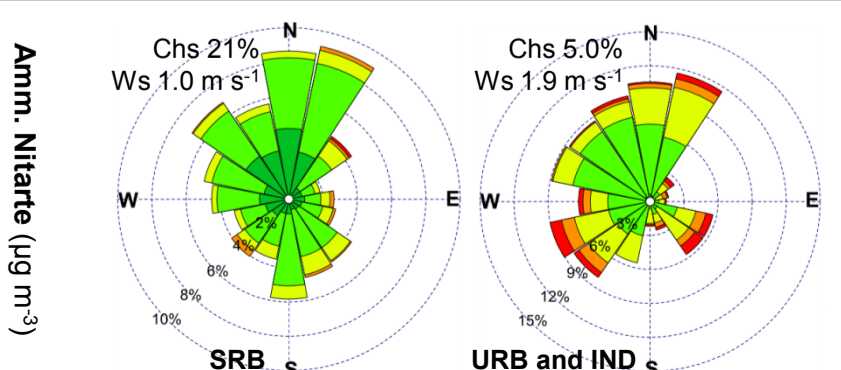
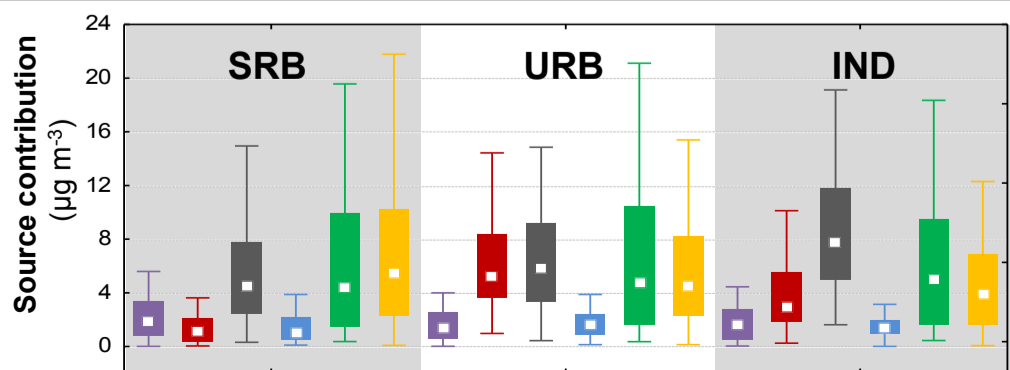
Group 3

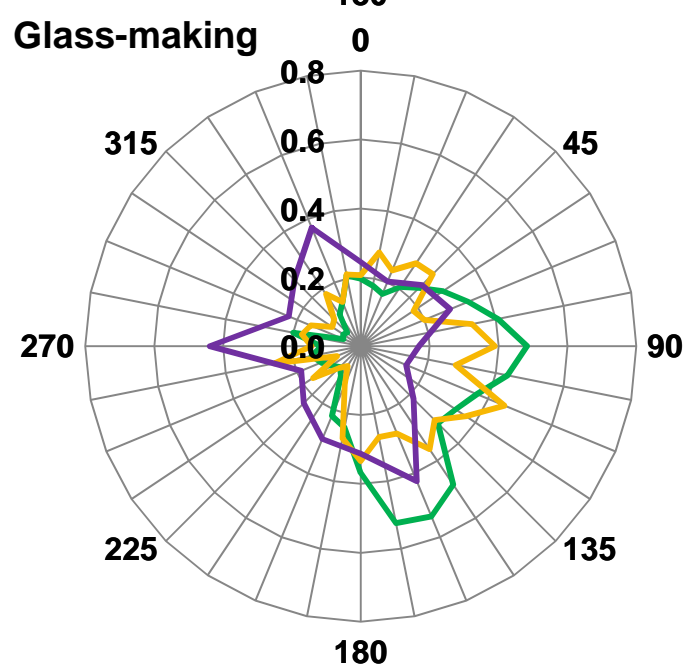
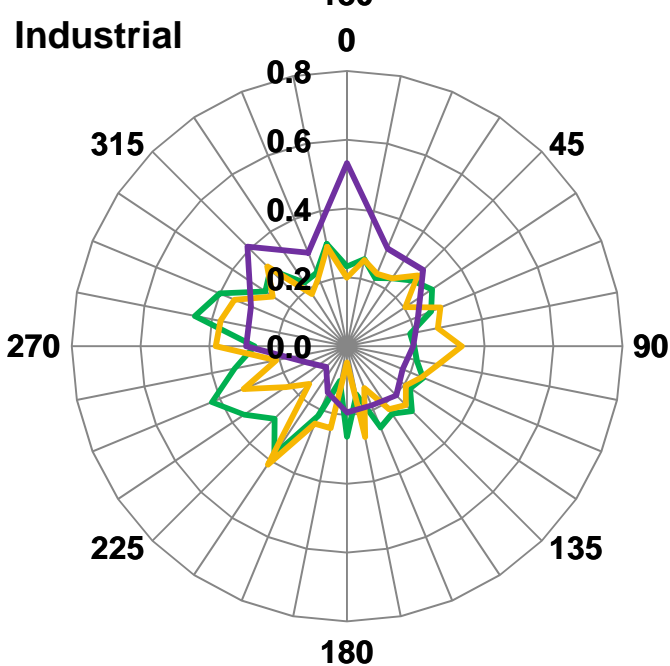
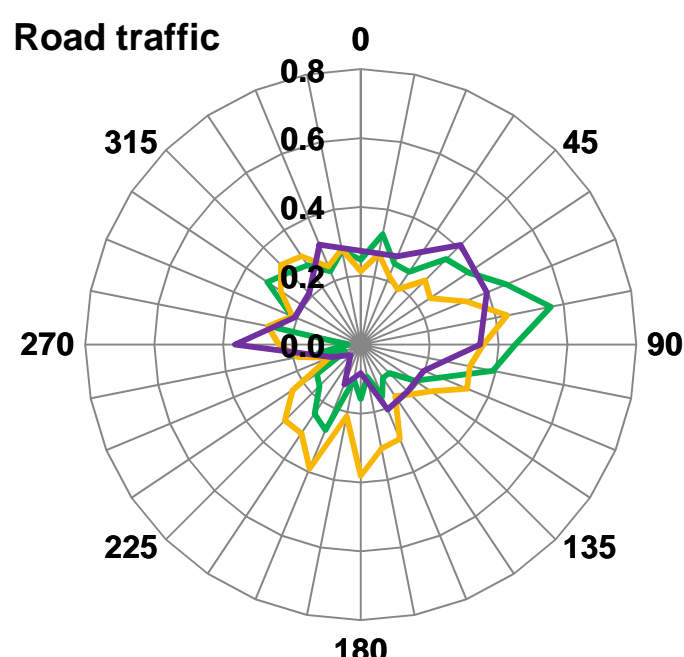
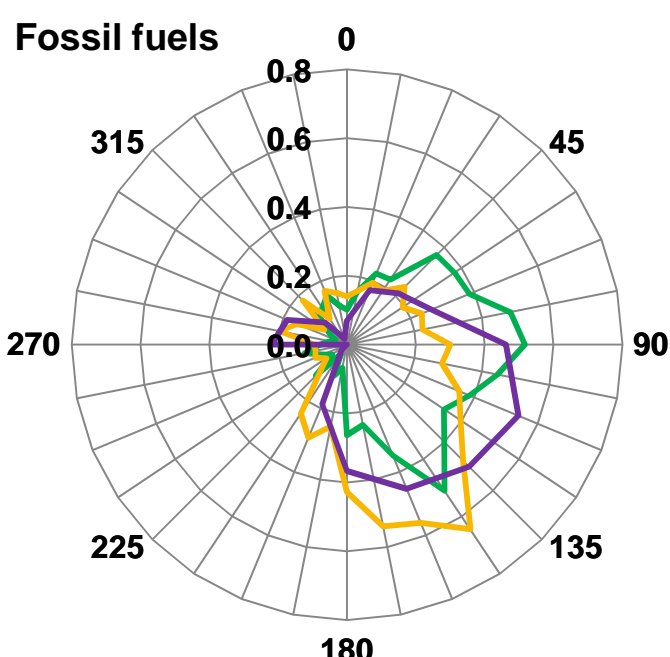
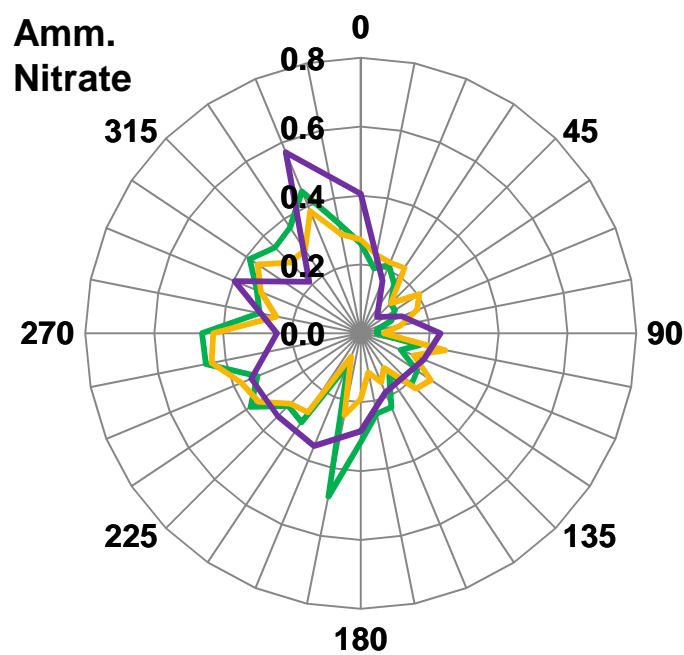
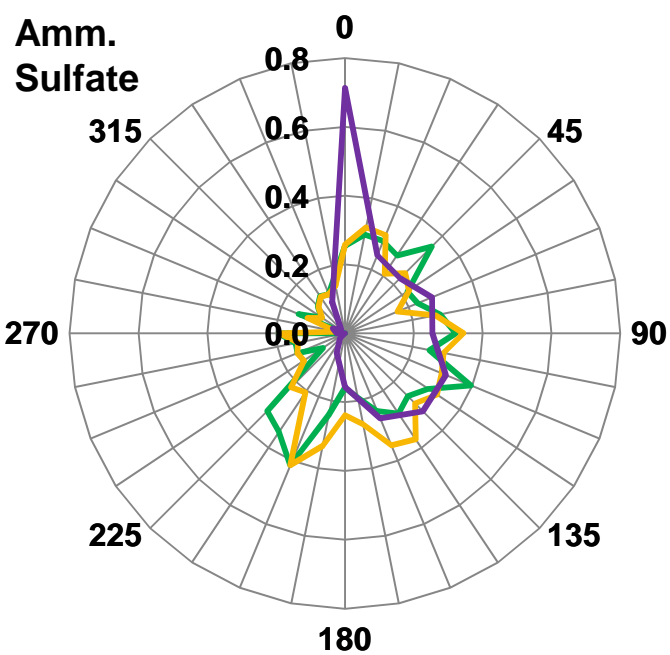


Group 4



Group 5





SRB
 URB
 IND

HIGHLIGHTS

- PM_{2.5} local and external sources have been evaluated in an European hot-spot area
- Meteorology-based methods have been applied to source apportionment results
- External contributions were evaluated applying Trajectory Statistical Methods
- Effects on PM sources of ground-wind circulation patterns were also investigated
- Local source contributions have been estimated following the Lenschow' approach

Cluster analysis on back-trajectories

The principal purpose of back trajectories clustering is to group trajectories having similar geographic origins and histories. The subsequent coupling of clusters with chemical data associated to air pollutants is a simple but powerful way to infer insights into the potential contribution of long-range transports from different pathways. There are several ways in which clustering can be performed several measures of the similarity (e.g., Carlslaw, 2015). The Euclidean distance (d) parameter is the most common technique used in a number of studies (e.g., Abdalmogith and Harrison, 2005; Owega et al., 2006; Borge et al., 2007; Markou and Kassomenos, 2010; Rozwadowska et al., 2010). It that can be defined as:

$$d_{1,2} = \left(\sum_{i=1}^n ((X_{1i} - X_{2i})^2 + (Y_{1i} - Y_{2i})^2) \right)^{1/2} \quad (\text{Eq. 1})$$

where X_1 , Y_1 and X_2 , Y_2 are the latitude and longitude coordinates of back trajectories 1 and 2, respectively, and n is the number of back trajectory points (96 hours in this case). In this study a non-hierarchical clustering method (K-Means) has been applied. The appropriate number of clusters has been selected by using the analysis of the total spatial variance (TSV), individuating when a large change in TSV occurs.

PSCF

The PSCF was initially developed to identify the likely locations of the regional PM sources (Lee and Hopke, 2006; Pekney et al., 2006) and calculates the probability that a source is located at latitude i and longitude j . The basis of PSCF is that if a source is located at coordinates i and j , an air parcel back-trajectory passing through that location indicates that material from the source can be collected and transported along the trajectory to the receptor site. PSCF solves:

$$PSCF = \frac{m_{ij}}{n_{ij}} \quad (\text{Eq. 2})$$

where n_{ij} is the total number of end points that fall in the ij th cell and m_{ij} is the number of end points in the same cell that are associated with samples that exceeded the threshold criterion (Carlsaw, 2015). The PSCF value can be interpreted as the conditional probability that concentrations larger than a given criterion value are related to the passage of air parcels through a grid cell with this PSCF value during transport to the receptor site (Hsu et al., 2003). This method is suitable for obtaining first knowledge of possible source regions (Dvorska et al., 2008 and references therein). Generally, PSCF values of 0.00–0.50 are considered as low, values of 0.51–1.00 are considered as high. In this study, PSCF has been calculated using the 75th percentile of source contribution as threshold criterion.

CWT

The main limitation of PSCF analysis is that grid cells can have the same PSCF values from samples of slightly higher or extremely higher criterion concentrations. As a consequence, larger sources cannot be distinguished from moderate ones. The concentration weighted trajectory (CWT) is a method of weighting trajectories with associated concentrations (Hsu et al., 2003). In this procedure, each grid cell gets a weighted concentration obtained by averaging sample concentrations that have associated trajectories that crossed that grid cell as follows, i.e. each concentration is used as a weighting factor for the residence times of all trajectories in each grid cell and then divided by the cumulative residence time from all trajectories (Hsu et al., 2003; Cheng et al., 2013):

$$C_{ij} = \frac{1}{\sum_{l=1}^M \tau_{ijl}} \sum_{l=1}^M C_l \tau_{ijl} \quad (\text{Eq. 3})$$

Where C_{ij} is the average weighted concentration in the grid cell (i,j) . C_l is the measured concentration (source contributions in this study), τ_{ijl} is the number of trajectory endpoints in the grid cell (i,j) associated with the C_l sample, and M is the number of samples that have trajectory endpoints in grid cell (i,j) . In summary, weighted concentration fields show concentration gradients across potential sources and highlight the relative significance of potential sources (Hsu et al., 2003).

CPF

The conditional probability function (Kim et al., 2003a; Kim and Hopke, 2004) analyses local source impacts from varying wind directions using the source contribution estimates from PMF coupled with the time-resolved wind directions. The CPF estimates the probability that a given source contribution from a given wind direction will exceed a predetermined threshold criterion. CPF is defined as:

$$CPF = \frac{m_{\Delta\theta}}{n_{\Delta\theta}} \quad (\text{Eq. 4})$$

where $m_{\Delta\theta}$ is the number of occurrences from wind sector $\Delta\theta$ (11.25 degree) that exceeded the threshold criterion, and $n_{\Delta\theta}$ is the total number of data from the same wind sector. To minimize the effect of the atmospheric dilution, the daily fractional contributions from each source relative to the total of all sources were used rather than the absolute source contributions (Kim et al., 2003a). The same daily fractional contribution was assigned to each hour of a given day to match the hourly wind data; hence 24 h was set as threshold criterion for $n_{\Delta\theta}$. Calm winds ($< 1 \text{ m s}^{-1}$) were excluded from this analysis due to the isotropic behaviour of wind vane under calm winds. The threshold

criterion has been fixed to the upper 25th percentile of the fractional contribution of each source according to most previous studies (Kim et al., 2003b; Kim and Hopke, 2004; Kim et al., 2005). The sources are likely to be located at the directions that have high conditional probability values (Kim et al., 2005).

References

- Abdalmogith, S. S., Harrison, R. M., 2005. The use of trajectory cluster analysis to examine the long-range transport of secondary inorganic aerosol in the UK. *Atmos. Environ.* 39, 6686–6695.
- Borge, R., Lumberras, J., Vardoulakis, S., Kassomenos, P., Rodríguez, E., 2007. Analysis of long-range transport influences on urban PM10 using two-stage atmospheric trajectory clusters. *Atmos. Environ.* 41, 4434–4450.
- Carslaw, D.C., 2015. The openair manual — open-source tools for analysing air pollution data. Manual for version 1.1-4, King's College London.
- Cheng, I., Zhang, P., Blanchard, P., Dalziel, J., Tordon, R., 2013. Concentration-weighted trajectory approach to identifying potential sources of speciated atmospheric mercury at an urban coastal site in Nova Scotia, Canada. *Atmos. Chem. Phys.* 13, 6031–6048.
- Dvorska, A., Lammel, G., Klanova, J., Holoubek, I., 2008. Kosetice, Czech Republic – ten years of air pollution monitoring and four years of evaluating the origin of persistent organic pollutants. *Environ. Pollut.* 156, 403–408.
- Hsu, Y., Holsen, T.M., Hopke, P.K., 2003. Comparison of hybrid receptor models to locate PCB sources in Chicago. *Atmos. Environ.* 37, 545–562.
- Kim, E., Hopke, P.K., Edgerton, E.S., 2003a. Source Identification of Atlanta Aerosol by Positive Matrix Factorization. *J. Air Waste Manage. Assoc.* 53, 731–739.
- Kim, E., Larson, T. V., Hopke, P. K., Slaughter, C., Sheppard L. E., Claiborn, C., 2003b. Source identification of PM2.5 in an arid Northwest U.S. City by positive matrix factorization. *Atmos. Res.* 66, 291–305.
- Kim, E., Hopke, P. K., 2004. Comparison between Conditional Probability Function and Nonparametric Regression for Fine Particle Source Directions. *Atmos. Environ.* 38, 4667 – 4673.
- Kim, E., Hopke, P.K., Kenski, D.M., Koerber, M., 2005. Sources of Fine Particles in a Rural Midwestern U.S. Area. *Environ. Sci. Technol.* 39, 4953–4960.
- Lee, J.H., Hopke, P.K., 2006. Apportioning sources of PM2.5 in St. Louis, MO using speciation trends network data. *Atmos. Environ.* 40, 360–377.
- Markou, M.T., Kassomenos, P., 2010. Cluster analysis of five years of back trajectories arriving in Athens, Greece. *Atmos. Res.* 98, 38–457.

Owega, S., Khan, B.-U.-Z., Evans, G. J., Jervis, R. E., Fila, M., 2006. Identification of long-range aerosol transport patterns to Toronto via classification of back trajectories by cluster analysis and neural network techniques. *Chemometr. Intell. Lab.* 83, 26–33.

Pekney, N. J., Davidson, C. I., Zhou, L., Hopke, P. K., 2006. Application of PSCF and CPF to PMF-Modeled Sources of PM_{2.5} in Pittsburgh. *Aerosol Sci. Technol.* 40, 952–961.

Rozwadowska, A., Zieliński, T., Petelski, T., and Sobolewski, P., 2010. Cluster analysis of the impact of air back-trajectories on aerosol optical properties at Hornsund, Spitsbergen. *Atmos. Chem. Phys.* 10, 877–893.

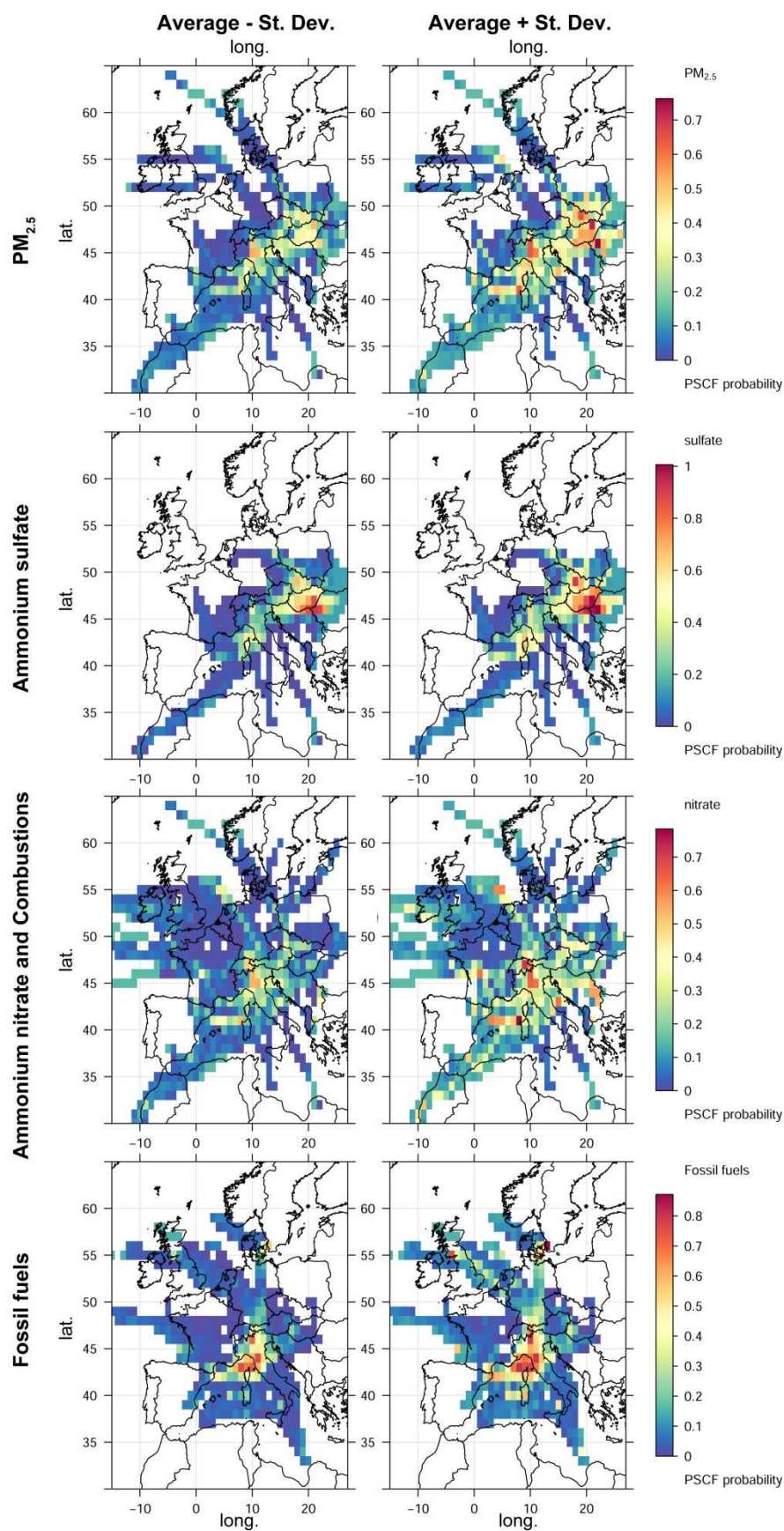


Figure SI1a. Associated uncertainties for PSCF expressed as average \pm standard deviation of $n=500$ bootstrap resamples.

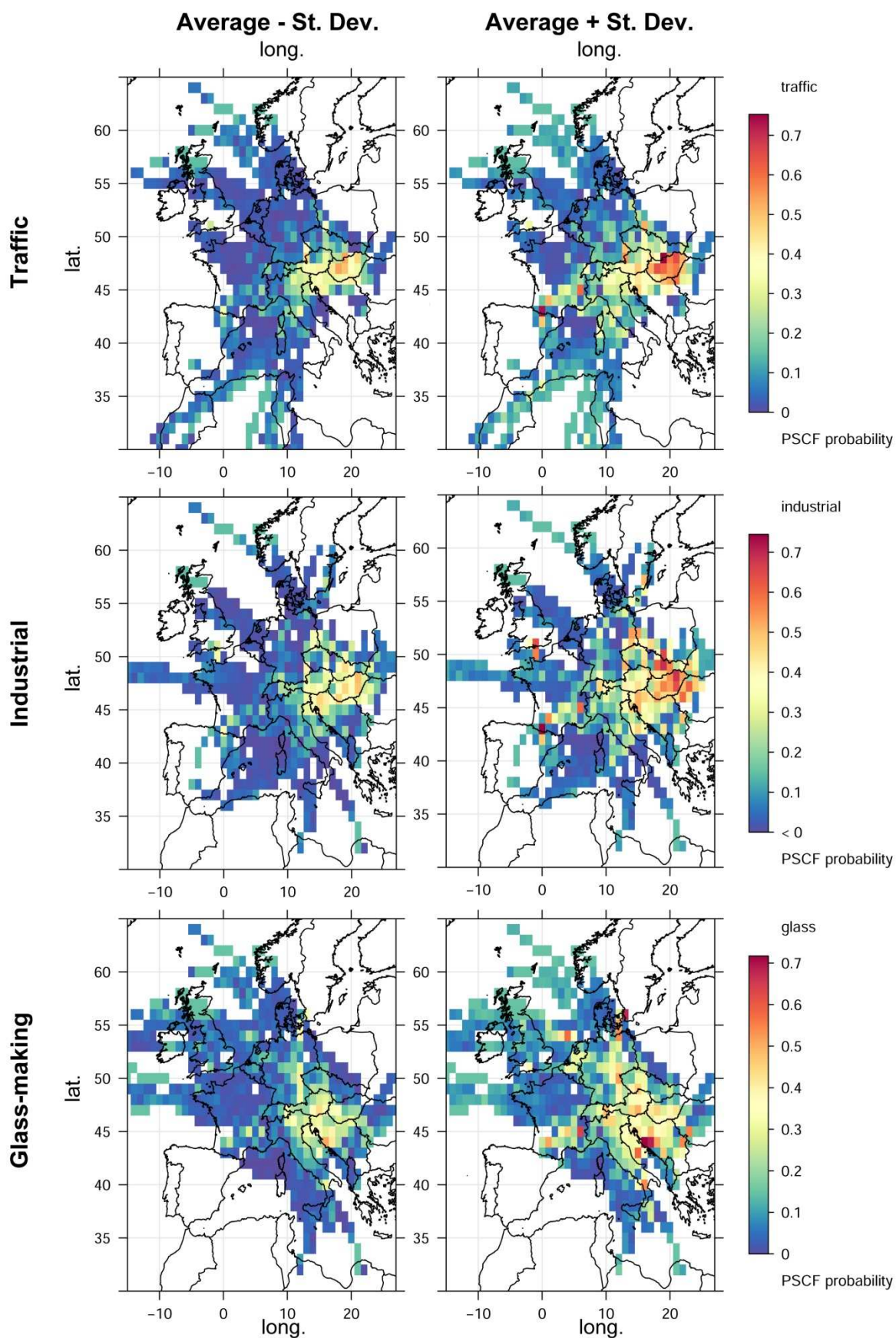


Figure SI1b. Associated uncertainties for PSCF expressed as average \pm standard deviation of $n=500$ bootstrap resamples.